CONTENTS

Research Articles

Research Article

RENEWABLE ENERGIES IN THE SETTLEMENTS
(A STEP TOWARD A CLEAN CITY)

Aidin ARMANFAR[1]* , *Mahsa KHANMOHAMMADI[2]*

[1] Student of architecture, Faculty of Art and Architecture, Yildiz Teknik University, Istanbul, Turkey
Orcid[1]: https://orcid.org/0000-0003-4931-6535
[2] Master of Architecture, Faculty of Art Architecture,Islamic Azad University, Tabriz, Iran
Orcid[2]: https://orcid.org/0000-0003-4720-6922
* Aidin Armanfar; a.armanfar.a@gmail.com

Abstract: *As a result of the energy crisis of fossil fuel in the world, and pollution that comes from using these types of fuels, humans need to find clean and affordable energy to survive, impelling communities which produce their energy to carry out new initiatives. The use of wind, water, earth, solar and other clean energy has become possible, and finally, the world is on a path that requires new research in this field. Between the urban and social elements, per capita energy in the housing sector is allocated the highest consumption in the world, and this sector has the greatest amount of energy consumption in Iran as well. Researchers are presenting new solutions in addition to the usage of technology in the production of renewable energies, making closer to reality the reproducible ideas about using parts of buildings and natural forces around the buildings. This study is an attempt to explore the surrounding natural forces and materials that are used in construction, alongside the study of books and valid and scientific global websites that discussing the idea of using new technologies along with the existing energy production. Using renewable energy, homes have been made from special materials, where the manner of design adjusts to the environment (like solar energy), but can still function in any condition. We have seen that by studying the available information, biogas and photovoltaic systems are also intended to (in addition to their own sufficiency) and lead to saving energy. The day is coming that single municipal buildings will manage to make their fossil energy usage reach zero.*

Keywords*: fossil energy, photovoltaic, biogas systems*

1. Introduction

The increasing mortality of fossil fuels, the push for diversifying energy sources, the development and energy security, and finally, environmental issues are all problems caused by the consumption of fossil fuels on the one hand , clean and reproducible sources of new energy are coming from the sun, wind, environmental conditions, and biomass methods on the other hand led to universal, serious attention paid to the development and expanded use of nuclear energy and increasing the share of the resources in the energy of world capacity. In this regard, in the architecture and design fields, they are emphasizing low consumption patterns, and most experts are wording towards these goals for buildings [1].

2. Materials and Methods

In this research, we examined the effort to produce maximum energy using the two methods: taking advantage of the Sun's light energy, and maximum biomass energy production by natural forces around the building. This small energy production pattern is to be used in the future public buildings of Iran. Because of the geographic position of Iran and Tabriz, the amount of radiation of the sun and the

perfect platform of this part of the world, we believed that there was a high percentage possibility of success of this goal [Author].

2.1. Biogas

Biogas consists of gases caused by the fermentation of animal and vegetable waste away from oxygen and produced by the effects of anaerobic bacteria activity that includes about 60 percent CH_4, a flammable gas, and rest of it consists of 30 percent CO_2 and a small percentage of N_2, O_2, H_2, H_2S and moisture. In some cases, biogas contains combinations of siloxane as well (Table 1). A remaining by-product is compost or organic fertilizer used in agriculture, prized for being rich in nutrients.

Table 1. The overall composition of biogas [Author]

The overall composition of biogas		
Percentage	**Formula**	**Combination**
50–75	CH_4	Methane
25–50	CO_2	Carbon dioxide
0–10	N_2	Nitrogen
0–1	H_2	Hydrogen
0–3	H_2S	Hydrogen sulfide
0–0	O_2	Oxygen

The main composition of biogas is methane, a flammable gas that composes between 60-70 percent. Methane is a colorless and odorless gas that if one kcal of it is burned, it, produces 252 cubic feet of thermal energy, which in comparison to other fuels, is a significant figure. Two other combinations, especially the hydrogen sulfide (H_2S) compound (which has a negligible contribution) is a poisonous compound. Another important advantage of methane fuel is that it does not produce toxic and hazardous gases like CO while burning, so it can be used as a healthy and secure fuel in home environments.

As previously mentioned, 60-70% of biogas is methane, and this high percentage of methane distinguishes biogas as an excellent source of renewable energy for succession of natural gas and other fossil fuels. Today it is used for heating factory boilers, in motor generators to produce electricity, home heating and cooking [2].

The use of biogas production in Iran is not a general application so far and is in the laboratory stage; while in the countries of Western Europe, Southeast Asia, and especially China and India, this technology is very impressive and these countries benefit by using this technology. Due to the diversity of existing systems in the producing of biogas, it is essential to look at specific examples of use. Here are a few cases that related to the final project:

2.1.1 The production pattern of household waste of biogas:

The overall structure of biogas machines has been established with two input and output ponds, a fermentation tank (hazm), and a gas tank that take into account different circumstances such as: weather, culture, economics and technology. In terms of the type and quality of the application, there are different systems in the world, and four common types are [3];

1. Biogas device floating is known as the pig model.
2. Biogas device with a fixed dome tank is known as the Chinese model.
3. Biogas device with a high ratio of length to width is known as the Taiwan model.
4. Anaerobic compost

The raw materials of biogas are organic wastes-plant, waste, animal waste, human waste and sewage plant sludge.

2.1.1.1 Biogas device with floating hood

This device is used widely in India and thousands of devices of this kind are producing power in India. Raw materials, after mixing with water, go from an input pond into the fermentation tank that is located underground, and after gas production, fermentation material moves to the outlet pond that is located on the side of inlet pond and productive gases are collected in the metal gas casing that is located on the reverse of tank openings (Figure 1,2).

The overall picture of this device is as follows:
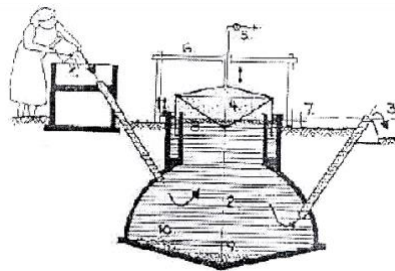
Figure 1. Biogas device with floating hood [4]. 1-Mixing tank with the entrance pipe. 2-Fermentation tank. 3-Weir flow from pipe output. 4- Tank holder of gas floating in liquid level . 5-Gas output with the bend of main pipe. 6-Help structure for a gas tank. 7-The difference of height equals to gas pressure of water in centimeter. 8-The floating layer of fiber when used as food. 9-Thick sludge. 10-Permanent layer of sand and rocks.
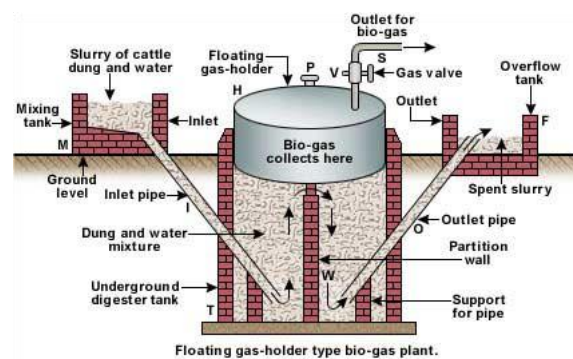
Figure 2. Biogas device with floating hood [5].

2.1.1.2 Biogas unit with fixed tank: (Chinese model)

Since these devices' origins are originally Chinese, the Chinese model is popular. This machine is built with a tank dome and underground gas tank fermentation is common due to fitting deep in the earth; this system increases efficiency in terms of savings in location and space needed and stabilizes the temperature and resistance of the device in cold areas which makes it important (Figure 3).

Thus, the gas chambers and fermentation are next to each other. A reservoir is built and the gas chamber is covered with a brick or concrete dome, and a valve is mounted on the gas tank. The Indian model is based on this device, but in this case the produced gas will climb the dome, and the pressure of gas production takes place when the consumption of fermented material in the discharge chamber propels the material exiting the outlet of the basin. This adjusts the gas pressure inside the dome, because

when the pressure increases, more material is removed. If the internal pressure is reduced during consumption, fermented material returns into the tank outlet valve to compensate pressure defects.
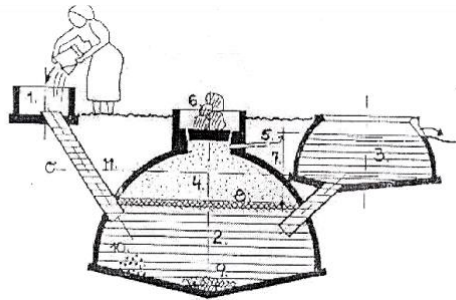
Figure 3. Biogas unit with fixed tank, (Chinese model) [6]. 1-Mixer with input. 2-Fermentation tank. 3-Outlet tank. 4-Gas holder tank. 5-Gas pipe. 6-Input plug (that is inhibited with the use of the weights). 7-Differences of height equal to the difference of water pressure in cm. 8-Clear layer. 9-Permanent layer of thick sludge. 10-Permanent layer of stone and sand. 11- Source line (zero) filling height of tank without gas pressure.

2.1.1.3   Biogas unit Taiwan model

This device can be built from different materials such as metals, PVC and fiberglass. The ratio of the length to the width in this system is large. The stream type is plug flow and hydraulic. Microbial retention time is the same due to the lack of returned mud, about 60 days (Figure 4).
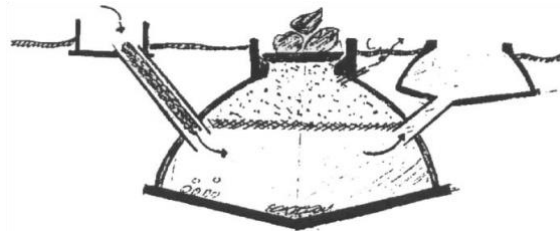

Figure 4. Biogas unit Taiwan model [7].

2.1.1.4   Anaerobic Compost:

Anaerobic compost is a sequence of processes by which microorganisms break down biodegradable material in the absence of oxygen. The process is used for industrial or domestic purposes to manage waste or to produce fuels. Much of the fermentation used industrially to produce food and drink products, as well as home fermentation, uses anaerobic compost.

Anaerobic compost is used as part of the process to treat biodegradable waste and sewage sludge. As part of an integrated waste management system, anaerobic digestion reduces the emission of landfill gas into the atmosphere. Anaerobic digesters can also be fed with purpose-grown energy crops, such as maize, this method is widely used as a source of renewable energy. The process produces a biogas, consisting of methane, carbon dioxide, and traces of other 'contaminant' gases. This biogas can be used directly as fuel, in combined heat and power gas engines or upgraded to natural gas-quality biomethane. The nutrient-rich digestate also produced can be used as fertilizer.

With the re-use of waste as a resource and new technological approaches that have lowered capital costs, anaerobic digestion has in recent years received increased attention among governments in a number of countries, among these the United Kingdom (2011), Germany, Denmark (2011), and the United States.
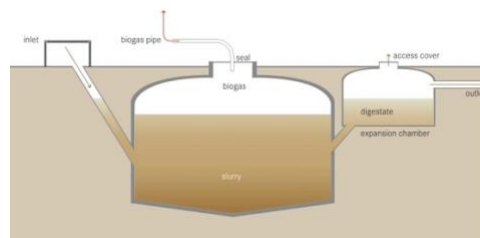
Figure 5. The Anaerobic Compost system for producing biogas [8].

2.2. The use of sun energy in the production of electricity (Photovoltaic Systems)

Solar energy is one of the broadest sources of renewable energy in the world. The energy from the sun falls on the Earth every hour, and exerts more than the total energy that the inhabitants of the Earth use in one year. To take advantage of this energy source, we should look to its scattered high efficiency and low cost to be converted to usable electric energy. In this method, by using specific technologies, energy is derived from sunlight to electrical energy conversion.

The condition caused by light radiation without using motion mechanisms that produces electricity is a photovoltaic phenomenon, and any system that uses this principle is called the photovoltaic system. A solar cell is a non-mechanical instrument that is usually made from a silicon alloy. When photons hit a photovoltaic cell, photons absorb energy to produce electricity. When the semi-conductor body, an object with a finite heat exchanges capability, absorbs the sunlight, the electrons of atoms of the object are moved. In order to build to a specific level, the object causes the front surface of the cell to attract electrons, So the electrons naturally migrate to the surface. When the electrons leave their position, holes are formed. Since the number of electrons is large and each one carries a negative charge to the front surface of the cell, load balancing between front and hind surfaces cannot maintain their balance, and an electric potential difference, like the positive and negative poles of a battery, is created. When the middle way between the two levels is -related, electricity is flowing. The use of photovoltaic panels in advanced countries is rapidly expanding. The photovoltaic panel in cases of cloudy weather can also produce electricity, although the output is reduced. In a very low light overcast day, a photovoltaic system may receive 5 to 10 percent of the normal days of sunlight, as a result its output as well as disseminate is low. The solar panel produces more power in the lower temperatures. Of course, PV systems, on winter days, produce less energy than summer days (Figure 6) [9].
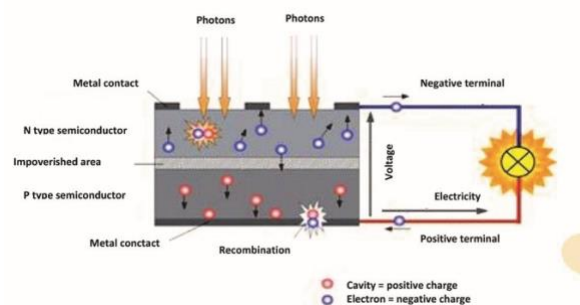

Figure 6. Analysis of the photovoltaic system [10].

Photovoltaic systems are one of the most consumed new energy applications. From the series and parallel cells, as long as there is sun, a reasonable voltage can be achieved. A collection of series and parallel cells are called a photovoltaic panel.

Generally, a photovoltaic system is composed of four main components:

1-solar panel
2-battery
3-power converter (inverter)
4-charge controller (Department of Electrical and Rural Energy Studies).

2.2.1 The solar panels in terms of the structure are divided into three major groups:

2.2.1.1 Polycrystalline solar panel

Multiple crystal solar panels or multiple silicon crystals are a key part of the solar panels' construction. These panels have lower lifetimes and prices compared to single crystal solar panels and are made from multiple crystal or silicon blocks that have less efficiency in absorption of solar energy compared to a single-crystal panel, but the cost of their manufacturing is lower. Use of them will be more cost-effective where space limitations are not an issue. This product is more appropriate for use in areas with dry climates [11].

2.2.1.2 Monocrystalline solar panel

Single crystal solar panels, in terms of history, are older than polycrystalline panels, but yields are higher than a few crystal panels. The single-crystal panels usually have a higher price and variations in manufacturing technology. According to the spatial limits on the solar system, these panels are more widely used, but this panel, due to fragility and hardness, should be installed and used in a more secure location. Ambient temperature is also a factor on the performance of this panel, that is, at temperatures above $50°$ C output drops appreciably (Figure 7) [12].
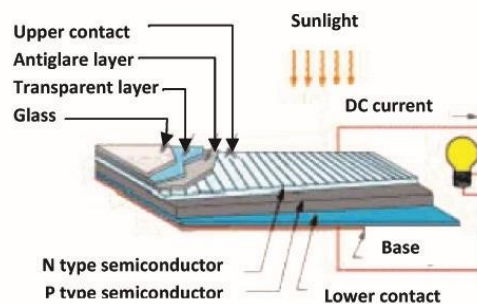
Figure 7. Analysis of the Monocrystalline cell [13].

2.2.1.3 Thin film solar panel

Thin-film solar cells, also called photovoltaic thin film cells, are solar cells of one or more thin layers of photovoltaic material on the layer below. This range in layers of thickness is very wide, ranging from a few nanometers to tens of micrometers. This product is for use in areas with more wet weather.
-Modules:
Each module usually has 20 to 40 solar cells that are connected to each other for series and parallel model. Each module has a maximum of 18 watts and the area is between 200 to 800 cm^2.
-Arrays:
A collection of photovoltaic modules and the retainer module frame for electrical or mechanical rides.
-Voltage regulation and control system:
Since the supply output electricity of the systems is DC, it should be turn out by the devices called inverter to AC, so that it enters the network.

-Energy storage in batteries:

Due to changing intensity of the sun's radiation during the day and in different seasons, it should be used in conjunction with a battery to save additional energy.

2.2.2 Photovoltaic systems use a variety of methods:

2.2.2.1 The grid connected systems:

In this way, the resulting electrical energy from photovoltaic systems' national network of power will be injected to the national grid (using direct current converter electric alternating current, such as the inverter connected to the network) In accordance with the specifications for the level of voltage, frequency, and phase difference.

2.2.2.2 The stand-alone systems:

This kind of application is able to provide the consumer required electric power energy without the need of a national network of electricity. In this way, the required electrical energy which can fit with high reliability can be installed and set up by using photovoltaic panels, storage and control systems, as a unit of power plants with a lifespan of 30 years.

Placement decisions of the panels in the roof of the buildings is located in the figure below:
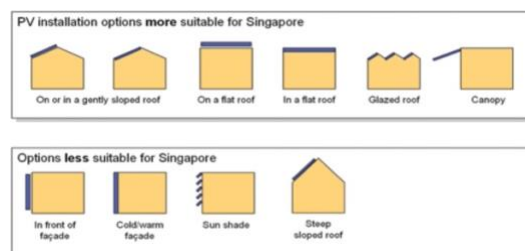
Figure 8. Placement decisions of the Panels in the roof of the buildings [14]

3. Results and Discussion

The selected systems in line with the production of renewable energy (Figure 9):

1. Photovoltaic system (monocrystalline solar 60 cell panel)

   The reason for choosing this model among the photovoltaic systems discussed in the article is its high efficiency, advanced manufacturing technology, easy installation and no need for much space. The photovoltaic system used in this building is a 60-cell monocrystal with dimensions of 100 x165 cm, and depending on the exact efficiency of the cells in them, they have an output of between 270 and 300 watts in standard conditions. Just a year ago, standard 60-cell panels were more like 250 or closer to wattage, but with advances in technology, the wattage of panels has increased to 300-350.

2. Biomass system (biogas)
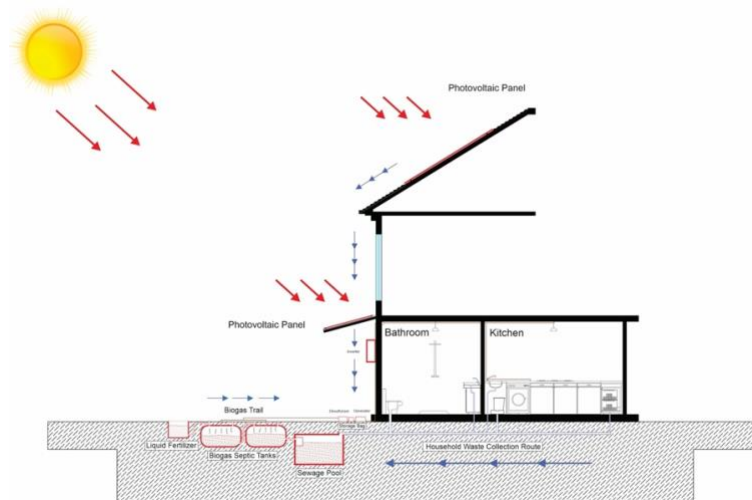
Figure 9. Selected systems [Author]

3.1. Photovoltaic system:

Solar panel energy is sent by light-sensitive cells to the electric voltage converter and then the energy is stored. Finally, it is necessary to use solar systems to load up electric charges. Based on the time it will be necessary to use an AC-DC inverter for AC loads and a DC-DC inverter for DC loads. In some of the systems (for the protection of the solar panel and batteries) it is also used as a charging control as well, which helps to avoid extra charges of batteries powered by the panel and also avoid draining batteries in the event that there is no production by the panel.

In household usage, this system well suits the needs of the building; furthermore, the possibility of storing the energy generated by this method is also available, which not only helps the building to be self-sustaining, but helps power requirements around building supplies as well (Figure 10, 11) [Author].
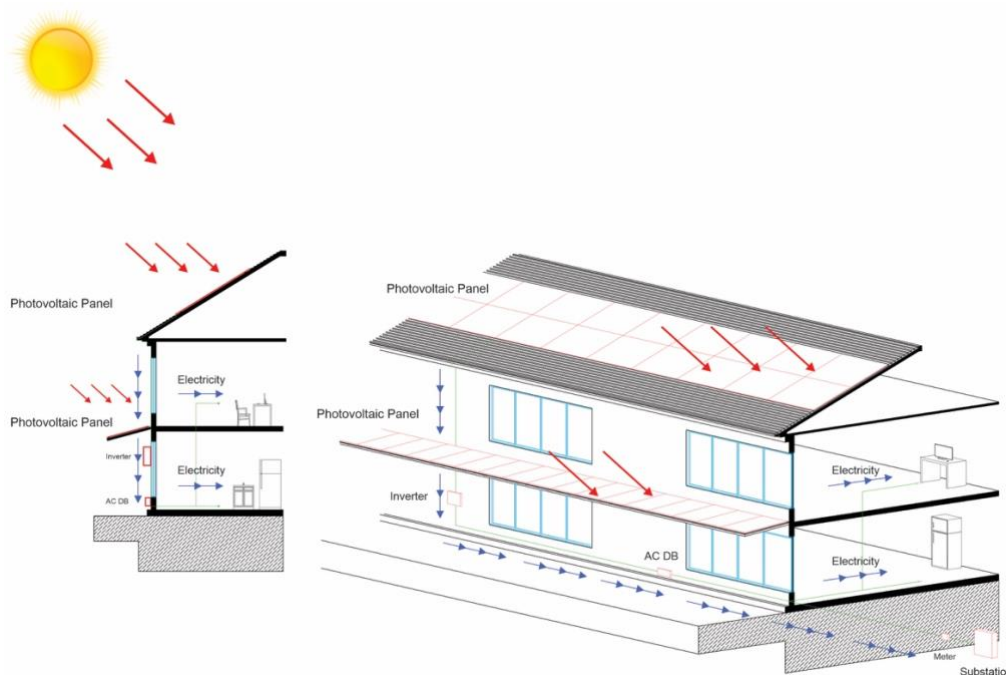
Figure 10. Overview of the photovoltaic system [Author]
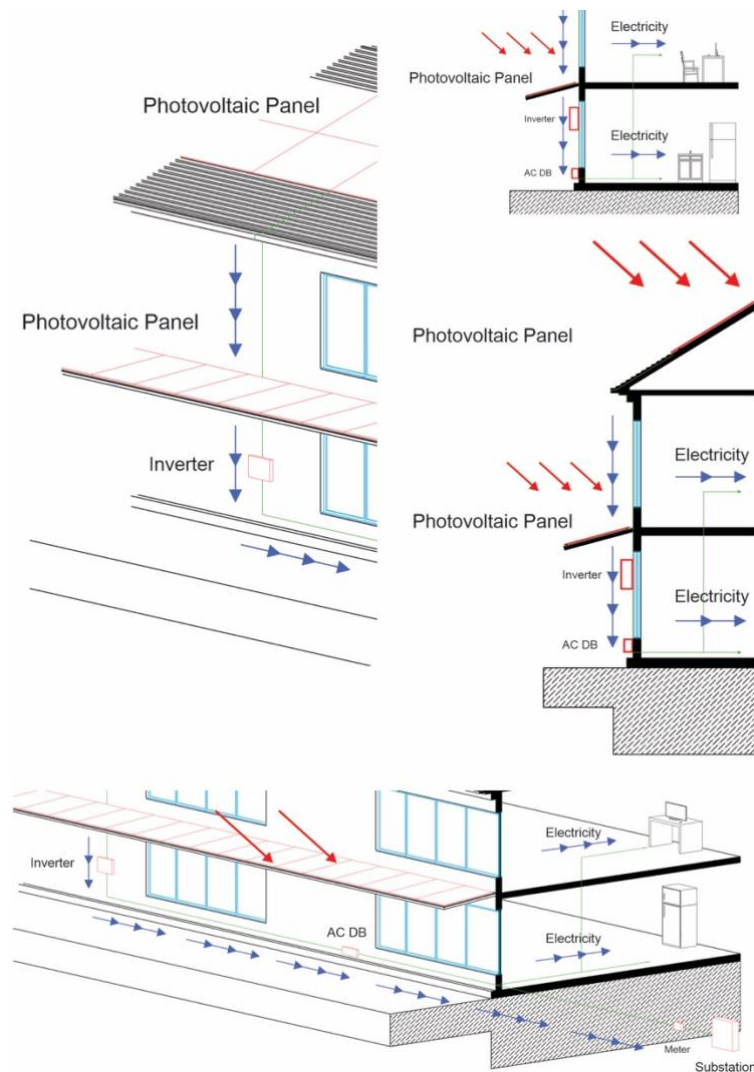
Figure 11. Large sections of the system [Author]

3.2. The biomass system (biogas):

This system collects all solids or liquids from kitchen wastes, which then go to the reservoir under the ground next to the building. Then these materials and fluids collected in the tank by the pumps to the tankers near the tanks. First, the material in the primary tank remains until the fermentation and the resulting gas from fermentation (biogas) has been redirected by the tube to the top and the sides of the desulfurize device. The resulting gas is then transferred to a storage container and then goes to the required places such as generator, electrical kitchen equipment, by pumps.

However, in the second part of the production phase in the preparation of biogas, the tank as shown in Figure 2, produces less biogas than first tank. The major product of this fertilizer tank is for gardening and agricultural use of the same house. In the final part of the above stages, non-potable and pretty clean water is obtained, which is also used in the building (Figure 12, 13) [Author].
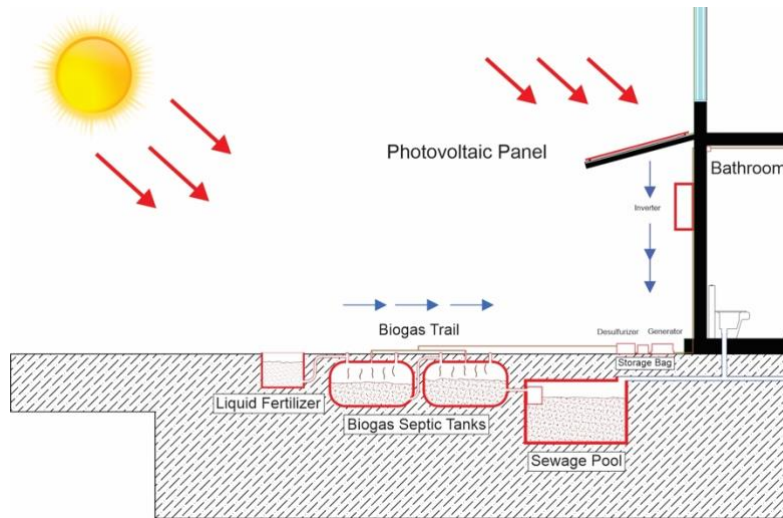
Figure 12. Section of designed biogas system [Author]
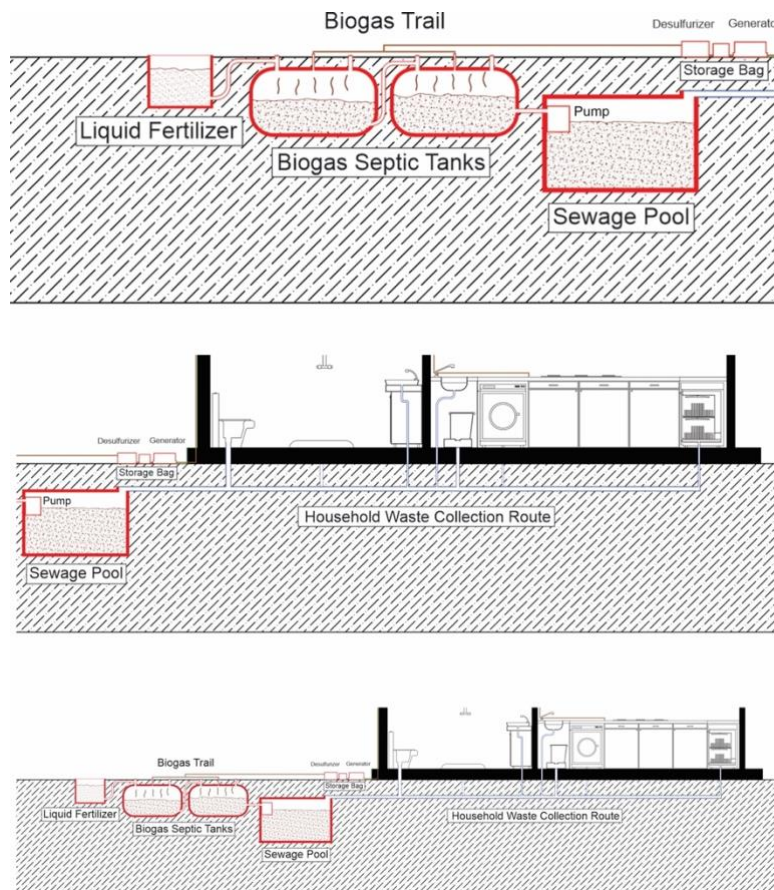
Figure 13. Zoom in biogas systems [Author]

4. Conclusion:

According to the systems and energies that were reviewed and tested in this research, we concluded the following:

1) Iran has vast resources for the production of biogas. With the usual values, the efficiency of biogas takes into account animal waste, waste of agriculture, urban sewage and garbage, and food industries and then applies the resulting coefficients. On average, biogas produces about 35/16146 million M^3, the equivalent of 323 petajoules of energy. Unfortunately, in spite of simple technology and productive potential of the biogas reactors, there is not a proper use of any of these sources in the country. Very few units exist due to the lack of proper guidance and administrative problems, and so do not have good efficiency [Author].

2) productive rural biogas uses animal manure digest, human sewage digest and three productive reactors of industrial waste. These numbers are in comparison with the number of units in the rural areas of biogas in India and Nepal (5000000, 2700000, 37000, 10) is liked at zero.

The most important factors in the development of biogas in Iran include:

1) Low energy prices
2) Lack of any specific reference to this type of energy
3) The lack of participation of the people and adequate training
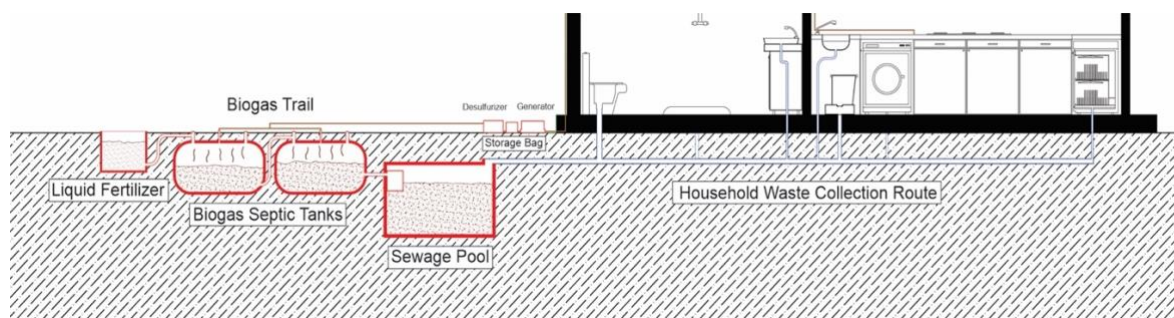
Figure 14. biogas system [Author]

Solar energy produces no carbon dioxide and is essentially limitless. Iran is located between 25 to 40 degrees north latitude and is located in an area that receives more direct sunlight than many other parts of the world. The amount of solar radiation in Iran has been estimated to be between 1800 to 2200 kilowatts per hour, which is of course higher than the global average. In the annual average, it is reported that more than 280 days are sunny in Iran, which is very impressive.

In this regard, the use of a photovoltaic system could be very fruitful in this climate and according to the facilities that this system puts in the amount of generating power at our disposal (production of electricity by the photovoltaic systems are usually 2-50 kilowatts), use of this system planning in the housing sector cannot fully free this community's consumption sector from fossil fuel dependency.

Properties of solar energies:

1) Solar energy is inexhaustible.
2) It is a clean energy and it does not cause damage to the environment.
3) Due to the lack of moving parts, it is easy to maintain.

4) It can fit the design to the capacity of the need.

5) It is a good fit with climatic conditions of Iran and has the ability to work in a wide range of temperatures and humidity.

6) It has low depreciation and high lifetime of structures [Author]

Authors' Contributions

A.A: Conceptualization, Formal analysis, Writing, Resources, Conclusion, Original draft preparation (60%)

M.K: Conceptualization, Methodology, Conclusion, Investigation (40%).

All authors read and approved the final manuscript.

References

[1] Islamic Republic of Iran Ministry of Housing and Urban Development, Atlas of Enerji, volume 2, Tehran: Planning Department, Ministry of Housing and Urban Development, 1994.

[2] Ghanavati H.and Tabatabaei M., Biogas, Fundamentals Process and Operation, Berlin: Springer-Nature, 2019, pp. 25-30.

[3] PlanET Biogas Solutions, 01 January 2016. [Online]. Available: http://www.planet-biogas.ca/biogas/info. [Accessed: 28 October 2019].

[4] Öztürk M., "Biogas Production from Animal Manure"[In Turkish] (2017). Available: https://docplayer.biz.tr/63615757-Hayvan-gubresinden-biogaz-uretimi.html. [Accessed: 26 August 2019].

[5] Saleh A., "Biogas potential in Pakistan," Renewable Energy Technologies, 5(10), pp. 5, 2012.

[6] Hejri Z. and Jami S. H., "Investigation of biogas production from wastwater and waste," *National Conference on Bioenergy*, Tehran, 2010.

[7] Telai A. R. "Biogas extraction technology from biogas production devices" (30 March 2007). [Online]. Available: http://www.knowclub.com/paper/?p=353. [Accessed: 22 April 2019].

[8] Anonymous, "Biogas Plant Sketch"(23 April 2018). [Online]. Available: https://i2.wp.com/thecityatlas.org/newyork/wp-content/uploads/Biogas_plant_sketch_ENG.jpg. [Accessed: 15 May 2019].

[9] Tabb P., Solar Energy Planning, Volume 1, Berlin: Print and bound by Halliday lithograph, 1980, pp. 53-70.

[10] Anonymous, "Renewable Energy" (01 June 2016). [Online]. Available: https://sites.google.com/site/obnovljivaenergijazauvijek/solarna-fotonaponska-energija. [Accessed: 13 May 2019].

[11] Europe Solar Production, (25 February 2018). [Online]. Available: http://www.europe-solarproduction.com/media/3051/poly-both_en.pdf. [Accessed: 25 June 2019].

[12] Dobrzanski L. A. , Macek M. and Drygała A., "Monocrystalline silicon solar cells," The Journal of Achievements in Materials and Manufacturing Engineering, 01(23), p. 12, 2012.

[13] Enis Photovoltaics, "Principle of Operation Photovoltaic Cell" (25 May 2015). [Online]. Available: https://www.enis-pv.com/en/principle-of-operation-photovoltaic-cell.html. [Accessed: 14 June 2019].

[14] Energy Market Authority (EMA) and the Building and Construction Authority (BCA), "Handbook for Solar Photovoltaic (PV) Systems", Singapore: EMA & BCA, 2012, p. 12.

Research Article

VIRTUAL POWER PLANT SOLUTION FOR KENYA RURAL ENERGY NEEDS

Obed Nelson Onsomu[1] , Bülent Yeşilata [2] *

[1]Ankara Yıldırım Beyazıt University, Graduate School of Natural Sciences, Ankara, Turkey
[2]Ankara Yıldırım Beyazıt University, Faculty of Engineering and Natural Sciences, Dep. of Machine Engineering, Ankara, Turkey
* Corresponding author; obedonsomu@gmail.com

Abstract: *A Virtual Power Plant system is an advanced power distributing and trading platform, that acts as a smart grid system unlike the existing conventional methodology of power allocation. The system is known to facilitate the connection of renewable energy sources to the national grid from a specific region, it is made up of Energy Storage System, Distributed Energy Resources, and Control System. Energy sources are classified as Distributed Energy Resources and various assets can be linked to the platform such as small-scale microgrids or community-based power platforms with demand-side management portfolios. A Virtual Power Plant platform has the power-distributing capability and an evolutionary trading platform (Peer to Peer trading). It has also proven to cut down carbon emissions as more renewables find their way to the grid. Additionally, data analytics and forecasting tools on the Virtual Power Plant are used to give information to the end-users on their storage, demand, and expected future generation. The user can interact with the system through a Human Machine Interface with an easy-to-use dashboard. Currently, the VPP systems have been implemented as pilot programs in countries such as Sweden, Norway, Belgium, and the USA. The potential application of the system can be extended as a case study and futuristic smart grid system for Kenya, as the National grid is substantially fed from renewable energy sources, and the vast majority of rural areas can benefit from cheap and affordable energy.*

Keywords*: Virtual Power Plant, Distributed Energy Sources, Rooftop photovoltaic, Renewable Energy Sources, Energy Storage Systems.*

1. Introduction

Kenya is located on the eastern part of the African continent bordered by Tanzania to the south and Uganda to the West. It has 582,650 sq kilometers and its location astride the equator enables Kenya to receive sunlight almost throughout the year. Average annual irradiation ranges from 4 to 6kWh/m^2-day and average sunshine duration varies from 5 to 7 hours a day depending on the regions. Kenya's installed capacity is 2,545MW as of July 2019, exceeding the demand figure of 2018 of about 1,802MW. However, the supply is not enough to keep up with the demand due to frequent network losses, droughts and renewable energy that varies with weather conditions from region to region. Out of the total installed capacity, the Independent Power Producers account for 991MW of on-grid capacity. In the year 2019, Kenya's energy mix was largely from renewable energy sources with an average of 86.8% of which 45% came from geothermal energy, which reduced thermal power dependence by 11% [1].

The country's energy reserves have diversified for the last decade and include petroleum, natural gas, coal, uranium, geothermal and Renewable Energy Sources including wind, solar and biomass as shown in Table 1.

Table 1. Total Energy Reserves 2019 [2].

Source	Installed capacity (MW)
Hydropower	820
Thermal generators	716
Geothermal	877
Wind	336
Solar PV	54
Thermal (gas turbine)	60
Off-grid and temporary thermal	57
Biomass	30
Total	2,950

The government has shown an increasing interest in the development of solar power plants across the country such as 50MW Garissa solar photovoltaic power plant which is a joint venture between the Kenya Rural Electrification (KREA) Authority and the Jiangxi Corporation for International Economic and Technical Co-operation (CJIC). Also, there are plans to step up power generation capacity to about 3,400MW from the existing 2,545MW for the next 5 years. Long term objective is to reach an installed capacity of 6,000MW within a decade. Solar and wind energy are less common energy sources, but through effective government policies investors have been motivated with fast bureaucracy and approval for on-site process. Projects below 3MW of solar power generation are permit free. There are about 150 commercial microgrids in Africa, whereby 65 of them are located in Kenya [3]. The expected number of microgrids in Kenya is estimated to be 2000-3000 in 2021, representing a huge market potential for microgrids. Diverse microgrids can be connected to the VPP platform, which provides a future market support platform for various energy actors especially renewables, and in the coming years renewable energy could replace fossil energy [4] , with implementation of this platform, new energy market systems will allow participation of consumers in trading, though, uncertainty of electricity price [5] could impede the adoption process. Research on mitigation of the uncertainty risk is suggested in [6] with emphasis on adjustment on confidence and robustness coefficients .Additionally, a cooperative optimal scheduling of energy resources has been studied in [7], and subsequent models have been suggested.

This paper focuses on the available energy mix in Kenya given that the country's economic growth has put pressure on electricity supply. Between 2004 and 2013, power demand rose by 18.9% annually. Therefore, VPP power sharing platform is suggested to connect rural areas that experience regular power outages or lack electricity due to distance from the national grid. Three households are modelled and assumed to be apart geographically (DER). Furthermore, the impact analysis of PV systems to the grid is analyzed and future work is suggested. Possible use cases for Kenya both as an emerging flexibility and trading concept are investigated. The model has been developed using MATLAB Simulink and MATLAB library components. Models of energy systems (such as energy storage, PV) and residential loads have been integrated and linked to the point of common coupling, the parameters used are solely for simulation purposes and they might not reflect the actual scenario of the Kenyan Grid network.

2. Previous Work

A VPP can be defined in various ways, it can be an aggregation of different type of distributed resources dispersed in different points of medium voltage distribution network. Additionally, it is a system that has flexible representation of portfolios of distributed generation units that can be contracted

in the wholesale market and offer services to the system operator. Lastly, as per the features and functions, it aggregates the sum of many diverse DERs to create a single operating profile from an amalgamation of various parameters characterizing each DERs, by incorporating the impact of the network on aggregate DERs output.
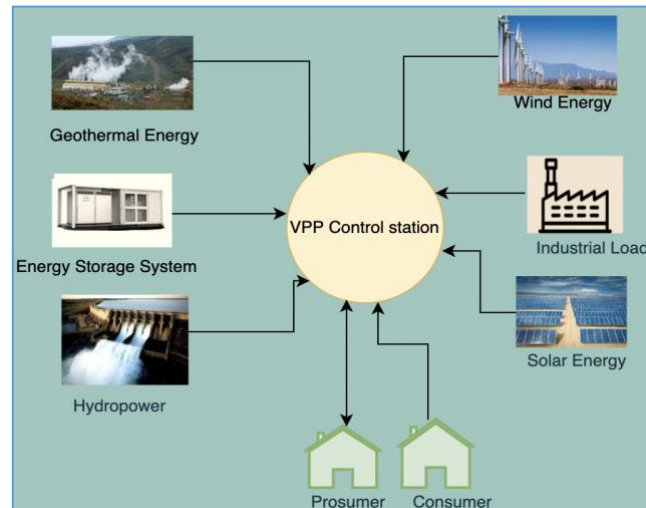
Figure 2. Large Scale VPP System for Diverse Renewable Energy Sources.

The system is composed of distributed energy resources, energy storage systems and a control centre for information management or information and communication Technologies as shown in Figure 2[8].

Distributed Energy Sources can be grouped into various categories depending on primary energy sources, capacity, ownership, and operational nature. In the first category, they can be wind-based generators, photovoltaic power plants, combined heat and power, biogas, and fuel cells (FC). As for capacity, these systems can be small-scale or both medium and large-scale capacity distributed generators. Regarding ownership, mostly the national government owns and operates these energy sources, but governments also encourage ownership by creating effective policies and licensing at the residential, commercial (Independent Power Producers DGs) or industrial level. According to the operational nature, DERs can vary with technologies based on wind, photovoltaic, FCs or micro-turbines [9]. Energy Storage Systems can store energy during off-peak period when the demand is low and give it off when the demand is high or during peak period.

Energy Management system coordinates and executes the commands between the DERs and existing loads, communication is bidirectional involving reception, control and forecasting of information of every component connected. Figure 2 demonstrates DERs in Kenya, more than 39% of electricity is hydro generated and are in most parts of the country. Geothermal energy sources are mostly located in a specific region (Olkaria), and Mega Solar power plant and wind-based energy sources are in Garissa and Turkana on the northern part of Kenya.

Table 2. Energy Demand Side Strategies and Technologies.

DSM Strategies	DSM Technologies
Community involvement	Pre-paid meters
Consumer education and village committees	Advanced metering systems with centralized communication
Price incentives	Conventional meters
Restricting residential use	Distributed Intelligent load controllers
Commercial load scheduling	GridShare
Efficient appliances and lights	Current limiters

Table 2 shows demand-side strategies in residential sectors as per government and other stakeholders' directives, this aims at fostering participation of consumers in the stabilization of the grid, and further lays a roadmap for future implementation of smart grid systems in the country [10]. For the VPP platform to be realized both consumers and prosumers play key roles in trading electricity power, as the latter can consume and generate power also termed as community-based small scale VPPs. In the case of large scale VPP, distributed generators or DERs require intensive capital investment as production capacity is within the range of 500-1000MW, which requires advanced system structures to control power flow by keeping up with the demand and dispatching DG resources on a timely basis, such kind of resources are not entirely switched off but are optimally controlled.

Table 3. Scheduling procedure based on priority [11].

Demand Priority	Remaining load 1	Remaining load 2	Remaining load 3
1st Priority	DG3(Hydro energy)	DG1(Geothermal energy)	DG2(PV)
2nd Priority	DG2(PV)	DG3(Hydro Power)	DG1(Geothermal energy)
3rd priority	GRID	GRID	GRID

Load scheduling and resource dispatch are given priority through control of active power for large scale VPP according to Table 3. Loads can be modelled as industrial loads attached to the grid network.

$P_{d(1,2,3)}$: Active power demand signal from load 1, 2 and 3.

$\Delta P_{d(1,2,3)}$: Remaining active power demand signal from load 1,2 and 3.

$P_{e(1,2,3)}$: Active power signal from DG 1, 2 and 3.

A limit is set for each load and when consumption is high and one single DG cannot cope with the supply a second DG is scheduled until all the DGs are used. In case the demand is not met by the available DGs, the grid power is scheduled. The process goes on repetitively ensuring steady power flow in the network, this is enabled by a communication and information module that collectively work to determine economical dispatch of DGs. The modules constitute a platform, in which data analytics, cloud computing and artificial intelligence functions are systemically accomplished, subject to low latency and high transmission performance [12].

2.1. Energy Management Algorithm

In this paper a central energy management algorithm is designed and the working of a local or household energy management has similar functionality. The energy algorithm has been designed for future use cases, control of renewables and storage systems for arbitrage energy trading, with focus on optimal dispatch of storage systems. It is assumed combined PV generation of households, energy storage systems and total load consumption are modelled as a unit and later extended into the grid

network through the point of common coupling, at this point the exchanged energy between the modelled microgrid and the grid can be monitored.
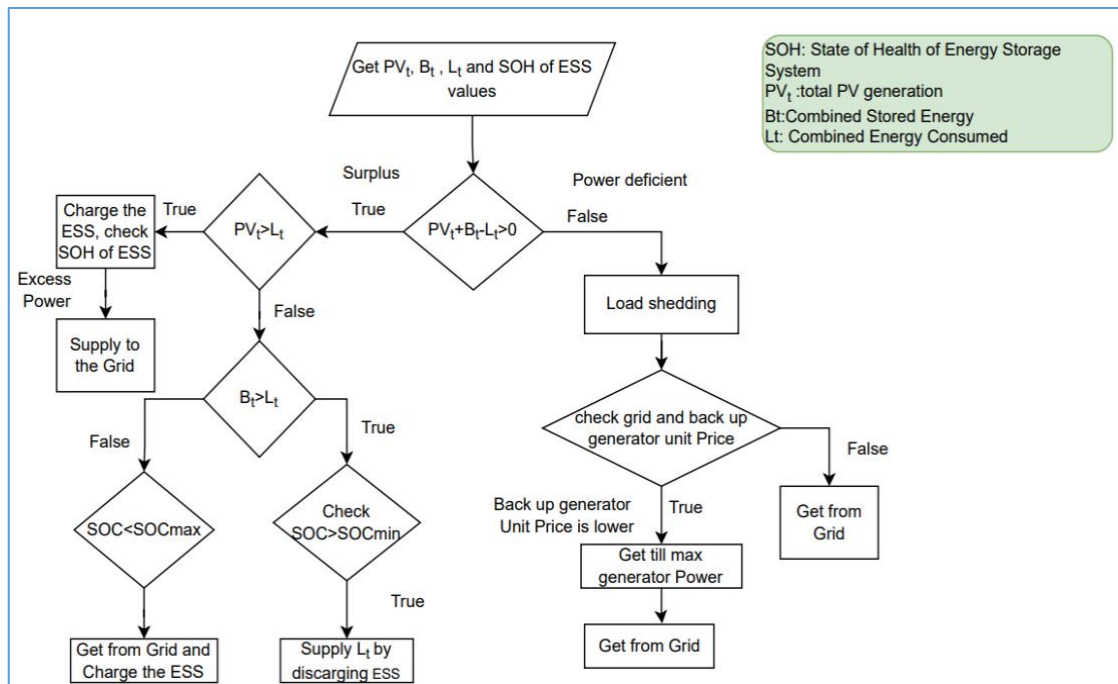

Figure 3. Energy Flowchart Algorithm

Figure 3 shows an energy algorithm flowchart that takes in values such as total Solar PV from the households, combined stored energy and total load consumption from the households under study. Depending on the energy balancing equation, an energy management system evaluates every part of the algorithm, if the output of the balancing equation is negative, then power deficit exists and the user is advised to apply load shedding, which reduces the amount of power consumed by altering non-critical consumption devices, this can either be by switching them off or changing the device settings. Additionally, the algorithm can check the prices of backup generator prices and compare them with the grid prices, and according to the energy needs of the households, the generator can supply maximum power and if power deficiency still exists, the grid can cater for the remaining power deficient.

On the hand if the balancing equation is positive, it implies surplus exists and both the battery and the total Solar PV have to be checked, in case total PV does not meet the households load demand, stored energy is checked and if true, state of charge is compared to the state of charge minimum to avoid over-discharging of energy storage system, if false, and it is found state of charge is less than state of charge maximum, then this ensures the energy storage system in not undercharged when supplied from the grid. In the instant that the Solar PV exceeds the household demand, energy storage system is charged by considering its state of health, after the cycle of charging, excess power is supplied to the grid, and the process continues.

3. Modelling and Simulation

Small-scale VPP is simulated using MATLAB Simulink 2021. Three households are connected to create a microgrid system that in turn forms an interface with the grid transmission system at a Point of Common Coupling (PCC). Each Household has a generation unit (Solar PV), Energy Storage System

and a load. Solar panels are typical technology tools and can be acquired and installed easily in many parts of the country.
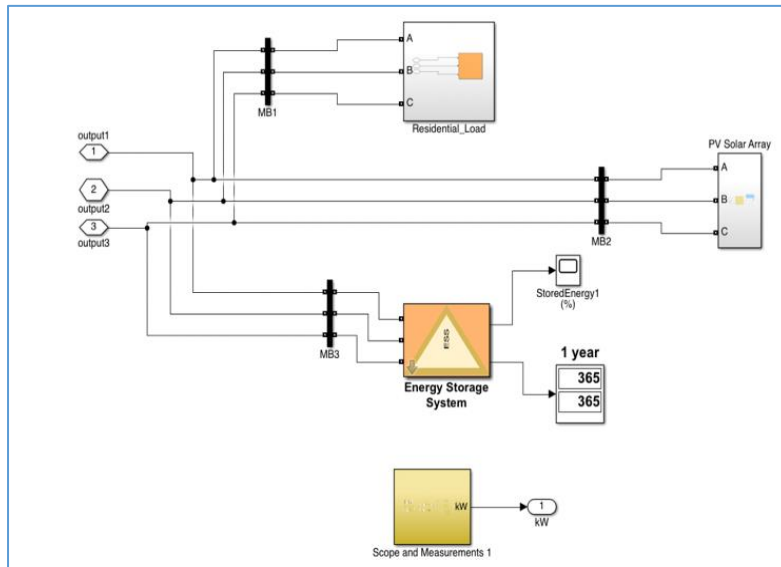
Figure 4. Energy Storage system, PV, and Load Household Simulink model
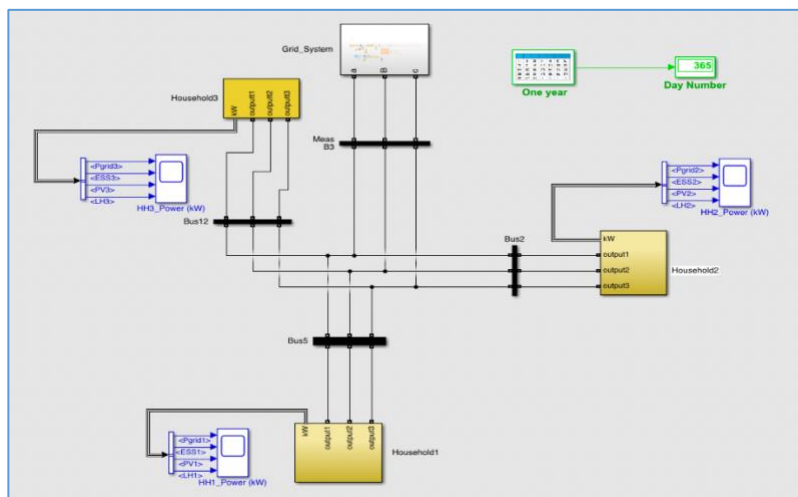
Figure 5. Three Households Grid-connected

Household structural arrangement of generational unit, Storage and load system is given in Figure 4 while MATLAB Simulink Model for VPP containing three households and grid is shown in Figure 5. The PV unit has a 20% efficiency and depends on the solar irradiance and temperature. In this study, Phasor simulation method is used, the simulation time is set to 365 days.

Table 4. Energy system components and capacities.

Energy system components	HH1	HH2	HH3
ESS (kW/kWh)	300/1500	240/1000	240/1000
Nominal LOAD (KVA)	1300	1500	1500
PV (kW)	220	200	1000

The battery has a capacity of 1000kWh for HH2 and HH3 with rated power of 240kW each, and the rated power for HH1 is 300kW with a capacity of 1500kWh. The rated capacity is set at 300kW for HH1 to monitor the impact of energy storage on the grid network. For each household, it is assumed that the load profile for HH2 and HH3 are the same 1500kVA each and for HH1 it is set at 1300kVA, while PV production for each household is also altered and studied as seen in Table 4. The maximum power that can be imported from the grid to the battery is 1000kW, and the grid transmission voltage is set to 120kV and is subsequently stepped down to 600V sufficient for this study.

4. Results and Discussion

Small VPP systems are interconnected as microgrids and then linked to the large scale VPP or the National grid, at the point of common coupling (PCC). The energy at the PCC increases due to the presence of ESS and PV generation systems that simultaneously import and export energy according to the household demand and solar irradiance.
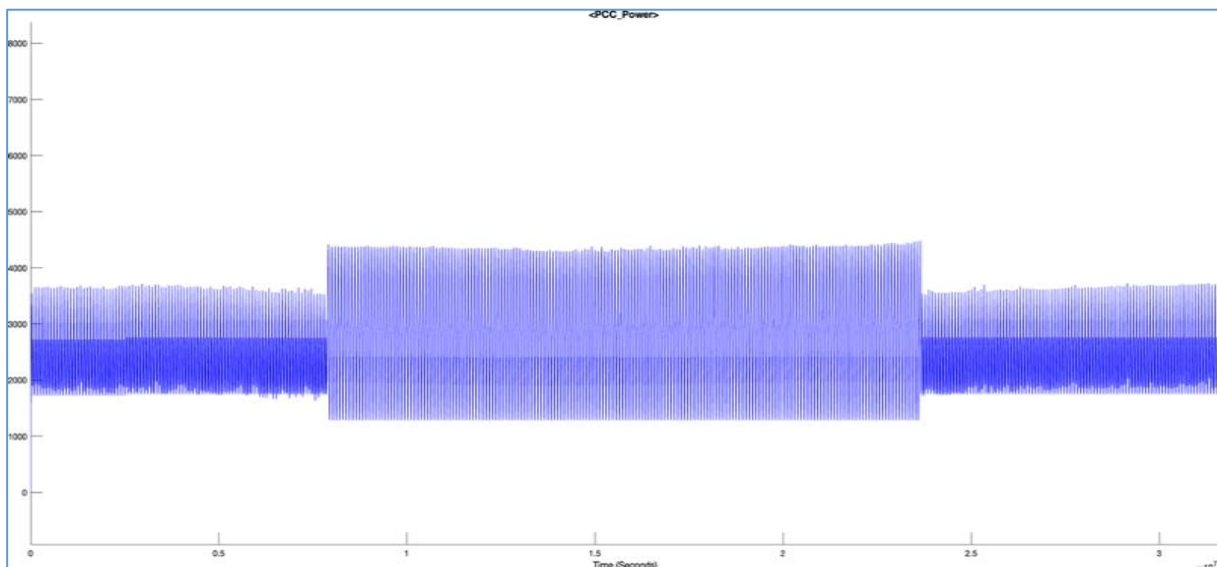
Figure 6. Power at the Main Point of Common Coupling

The resultant power at PCC (kW) is shown in Figure 6, for the first three months there is power variation and households do import energy from the PCC, and therefore maintains a profile of about about 3800kW, which later rises to about 4800kW for the following six months due to high solar irradiance experienced, and the PCC profile continues steadily until Solar PV output decreases as cooler months are approached, which explains the sudden decrease of power at the main PCC, a state that is quantified by more power exchange between the grid and the modelled microgrid that imports grid power to a large extent to cater for the household demand.
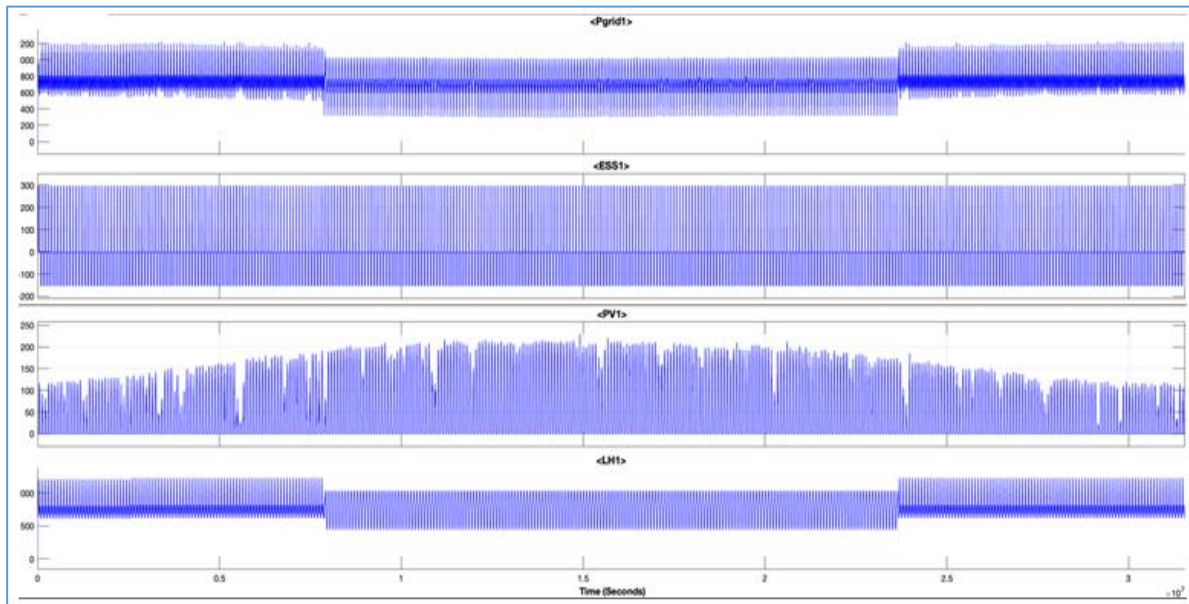
Figure 7. Household1 ESS1, PV1, LH1 Power Profile

Household1 shows that consumption decreases after the first three months, which also has an impact on the grid as more power is imported from the grid, the ESS has constant charging and discharging cycles, impliying maximum use of the ESS, there is surplus power as the load consumption for household 1 decreases slightly below 1000kVA, more power is stored with an approximate charge rate of 300kW, and PV output decreases slightly below 100kW towards the end of summer. Finally the ESS system stabilizes the grid by steadily supplying the load with an almost constant charge rate, Figure 7.
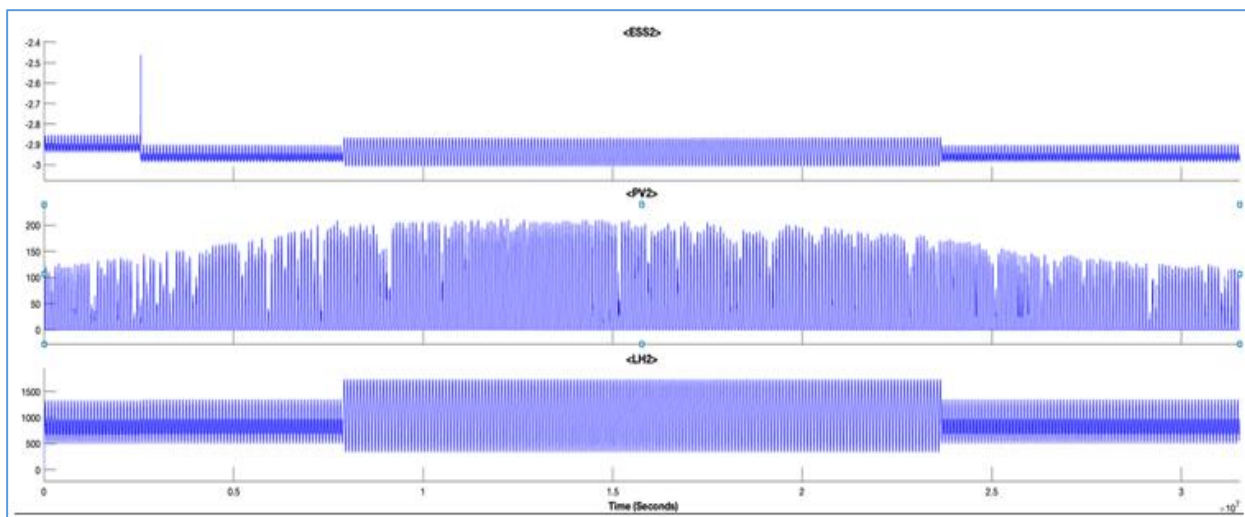
Figure 8. Household2 ESS2, PV2 and Load Power Profile

Figures 8 shows energy dissipated from the ESS, PV, and consumed energy by the load, and represents HH1whose ESS shows a declining energy profile in kWh as most of it is fed to the grid and the rest is consumed by the load. For the PV, Energy increases because of increased irradiance throughout the months, the beginning of the first three months, there is Solar PV output of about 120kW which is the amount of energy consumed by the load and stored, overtime Solar PV hits a record of about 150kW at the same time the ESS is maximumly discharged to an approximate value of 2.85kW, and further discharged to 2.9kW as Solar PV output decreases to about 100kW. In the meantime, the

load consumes maximum power of about 1500kVA during maximum Solar PV output, which explains sharp discharge of ESS to extensive negative values, and the consumption of 1400kVA continues irrespective of the status of the ESS, a challenge that is caused by over-discharging of the storage systems, this can be rectified by application of a robust energy management system techniques.
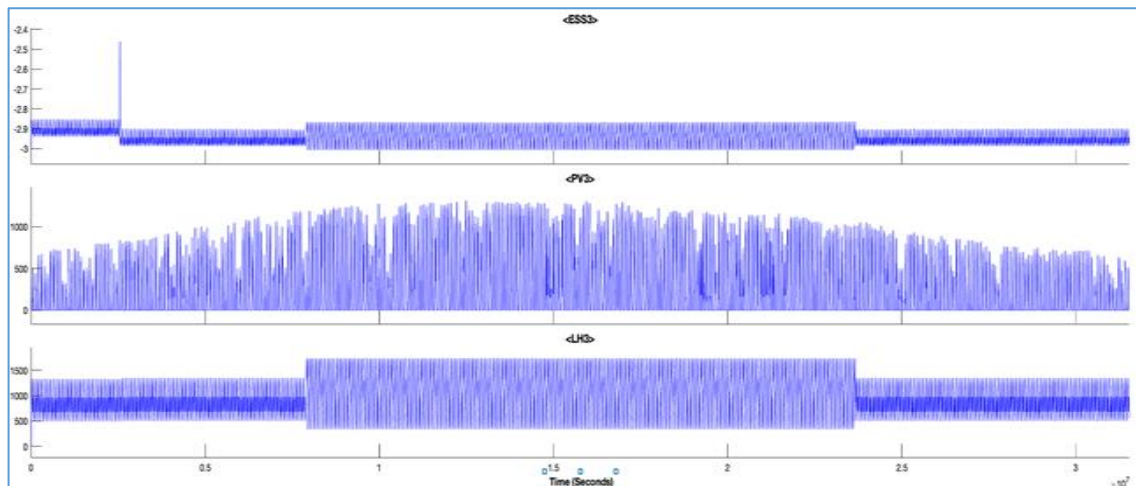
Figure 9. Household 3 ESS3, PV3 and Load3 Power Profile

In the case of Figure 9, Solar PV output is about 500kW for the first three months and later rises to about 1000kW as maximum, the previous households Solar PV output ranges between 100kW-150kW as minimum and maximum obtainable outputs. This implies the charge rate of ESS has to be increased to cater for more energy and both charge and discharge constraints have to be included, so as to avoid quick discharge cycles due to excess power demand from the load and Solar PV output intermittency that causes uncertainty in power output, causing a continuous discharge phenomenon of the ESS to about 2.9kW. The load is maximumly catered for, and in the first three months it consumes 1400kVA and takes a sharp increase to about 1500kVA, uncontrolled nature of the load results in extreme consumption of energy creating a completely unbalanced grid network, and violation of energy balancing equation as shown in Figure 3.
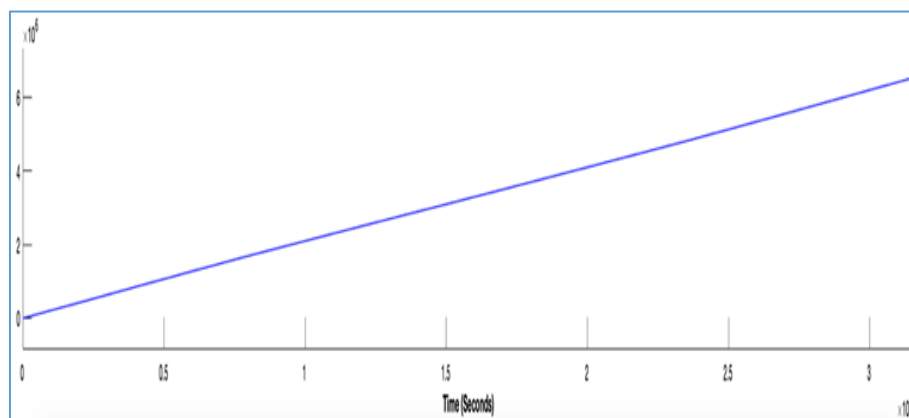
Figure 10. Energy (kWh) at the Point of Common Coupling

The beginning of January is characterized by low irradiance, the PV output is insignificant and most power is supplied by the grid at an average of 200kWh, but towards summer the output of PV increases and the amount of energy drawn from the grid decreases, which shows a typical value of around 600kWh available at PCC, this amount is quite large due to the Solar PV surplus at the household level that can easily cater for the demand and at the same time be stored in respective energy storage systems.
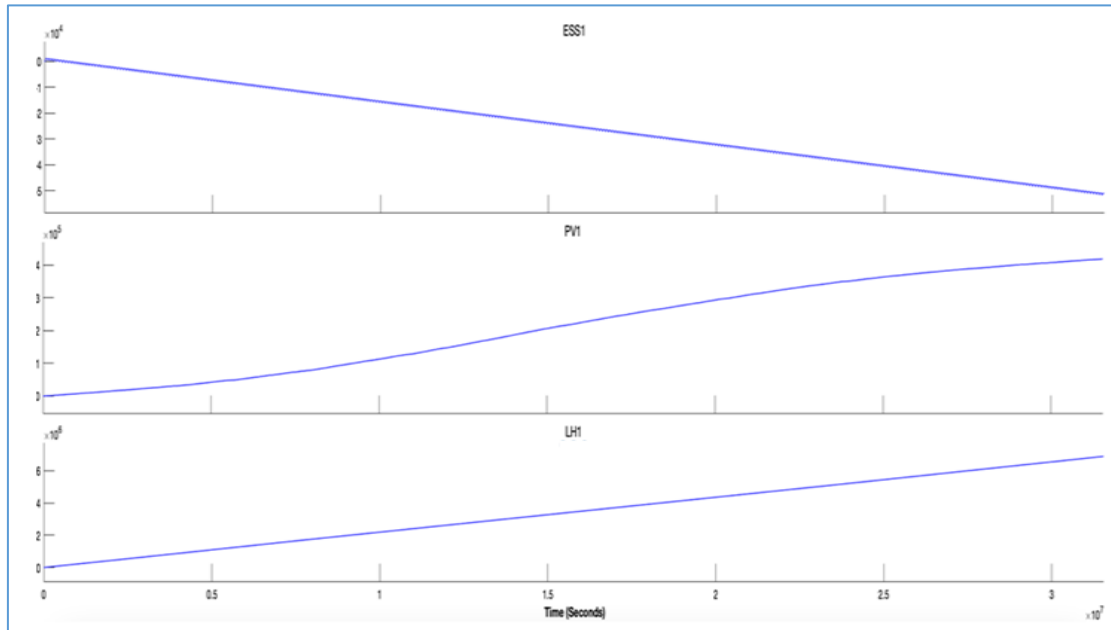
Figure 11. Energy kWh Variation for Household1

Energy (kWh) can be represented by using HH1 for this study. Energy at the PCC steadily increases, and the ESS shows a declining trend to almost -40kWh, meanwhile PV generation shows a positive generation to a maximum of about 300kWh and finally the load indicates consumption is in the upward trend and almost reaches 500kWh in Figure 10 and 11. The upward trend is due to the incoming energy supply from the battery and the Solar PV output, both energy supply systems boost the load consumption profile as evidenced in LH1 of Figure 11.

The discharge circle is quick especially for HH1 which is about 300kW maximum, as the load consumption drops during summer, excess power is stored and discharged to cater for the load consumption at the same time export to the grid, at the beginning of the first three months due to less PV generation the load consumes about 1250kVA partially from the grid power and the ESS power, as Solar PV output increases steadily the load later drops to 1000kVA following the start of April, the PV generation steadily increases but power at Pgrid1as shown in Figure 7 also decreases to about 1000kWh, implying more PV power is stored and consumed rather than be imported from the grid, which explains the bulging nature at the main PCC.

 HH2 and HH3 as shown in Figures 8 and 9 have a similar trend in the load consumption pattern, but the difference is exhibited in the Solar PV output which creates power imbalances for the households, HH2 ranges between 100-150kW of PV output, for HH3 the large penetration of Solar PV creates excess intermittent power in the range of 500kW-1000kW with the storage capacity of 1000kWh used for this study. The load consumption is 1400kVA at the beginning of the first three months, and then rises to a maximum of about 1500kVA towards the end of summer, which creates an unbalanced

power for the households and later over-discharging of storage system, which can be lethal in real physical systems, i.e., fire break out, reduced storage efficiency or even explosions. Additionally, the loads especially for HH1 shows more energy consumption of about 1000-1250kVA, at the expense of the available storage capacity of 1500kWh (charge rate of 300kW), and the generation of Solar PV that stands at 220kW maximum.

To have a more stable and well-balanced grid system and avoid uncertainty, more robust system controllers must be implemented to manage output of Renewable Energy Sources (RES), and similarly excess energy should be channeled to the storage systems. According to the simulation, addition of more PVs leads to unforeseeable technical challenges and actors such as storage systems should be properly sized to avoid undercharging or over-discharging challenges, hence energy must be managed to ensure the health and safe operation of storage systems and maintain grid stability.

The demand has to meet supply all the time, which physically implies ensuring generation output does not exceed the demand and the ESS can store and export without being over-discharged for optimal performance of the grid network, research that is out of the scope of this paper.

Use Case for Kenya:

The ESS has a storage capacity of 1000kWh. It is to be synched with the generation unit of individual households and 100% charged at rest. ESS couple to VPP system are mostly fitted with charge controllers, amount to be dispatched is pre-determined to guarantee storage for a longer period. Therefore, a prosumer can decide to trade the remnant power after meeting household power demand, through selling the remaining power to utility service provider or the KPLC state-controlled company, to be enabled through usage of smart metering systems that measure, record, send and forecast future electric demand and supply. If generation units meet the demand of the household but fail to store more energy, the consumer is relieved from incurring any extra cost.

If the demand supersedes generation, households must supplement their demand by importing from the grid and incur slightly less charges than the normal tariffs charged by the utility company, and both the storage and PV output will cater for most of the household demand. Kenyan diverse payment platform M-Pesa is the most used platform for sending and receiving money. Therefore, through incorporation of smart meters with M-Pesa till numbers and finally with VPP, automatic transactions can be actualized in real time for users trading power to the grid, and in return they will receive less charges depending on their household demand.

VPP plants in Kenyan energy sector can also be extended to serve rural settlements. The state can easily offset charges for energy poor settlements as monitoring of wide range of microgrids can easily be assessed and controlled through the Information Computer Technology component of the VPP, an initiative that can boost small medium enterprises.

5. Future Work

Following subjects can be considered as future works:
- A study on how to maximize the profit of VPP for rural poverty eradication program.
- Optimization techniques in handling multiple microgrids connected to the VPP platform.
- Developing an energy management tool for the households and determining charge and discharge levels for households.
- Re-modelling the households and power analyzers to adopt Kenyan M-Pesa transaction platform for trading and rural electrification programs.

6. Conclusion

The household model has been developed in MATLAB, and power profiles for the households have been analyzed. The effects of adding renewables to the grid system are apparent as consumption from one household to another changes, and therefore an energy management system is suggested for future work. Additionally, the model can act as a baseline for Kenya to lay the digital blueprint for futuristic VPP trading platform. The Kenyan payment platform M-Pesa can help commercialize VPP systems across the country. Also, a VPP solution for Kenya energy needs especially for people living in rural areas can facilitate rural electrification programs through cheap and affordable electricity.

Finally, adoption of VPP can eliminate the negative economic impact caused by power outages for investors and various manufacturing sectors, and enable consumers to participate in production of power, the presence of energy storage systems will also boost participation in arbitrage trading.

Acknowledgement

References

[1] Society for International Development (SID) "Energy For What ? Contemporary Energy Issues & Dilemmas in Kenya" (December 2021) [Online] Available: https://ke.boell.org/en/2021/12/14/energy-what

[2] IASS/SERC, Status and trends of energy development and climate action in Kenya, COBENEFITS Impulse. Potsdam/Nairobi. 2021 [Online] Available: https://www.cobenefits.info/wp-content/uploads/2021/07/COBENEFITS-Impulse_Energy_Climate-Action_Kenya.pdf

[3] Duby S. and Engelmeier T., Kenya: The World's Microgrid Lab, TFE Consulting, München , 2017.

[4] Wen Y., Yang W., Wang R., et al. Review and prospect of toward 100% renewable energy power systems[J]. Proceedings of the CSEE,2020,40(06):1843-1856.

[5] Liang Y., Zhou Q., Pan Y., and Liu L., "Risk Stabilization and Market Bidding Strategy of Virtual Power Plant Alliance Based on Multi-stage Robust Optimization," in *2022* 7th Asia Conference on Power and Electrical Engineering (ACPEE), Hangzhou, China, Apr. 2022, pp. 351–356. doi: 10.1109/ACPEE53904.2022.9783960.

[6] *2020 5th Asia Conference on Power and Electrical Engineering (ACPEE)*. IEEE, 2020.

[7] Chengcai W., Jian X., Shanxian L., et al. "Two level scheduling model of virtual power plant with constant temperature control load and renewable energy" . Applied energy, 2018, 224:659-670.

[8] Zhang Y., Pan W., Lou X., Yu J., and Wang J., "Operation characteristics of virtual power plant and function design of operation management platform under emerging power system," in 2021 International Conference on Power System Technology (POWERCON*)*, Haikou, China, Dec. 2021, pp. 194–196. doi: 10.1109/POWERCON53785.2021.9697609.

[9]   Mahmoud O., & Hegazy, Y.G. & Almoataz A. (2015). A Review of Virtual power plant Definitions, Components, Framework and Optimization. International Electrical Engineering Journal (IEEJ). 6. 2010-2024.

[10] Kiprop E., Matsui K., Karanja J. M., Andole H., and Maundu N., "Demand Side Management Opportunities In Meeting Energy Demand In Kenya." Japan Council for Renewable Energy, 2018. doi: 10.24752/gre.1.0_18.

[11] Onsomu O.N. and Yeşilata B., 'Virtual Power Plant Application for Rooftop Photovoltaic Systems,' 2019 3rd International Symposium on Multidisciplinary Studies and Innovative Technologies (ISMSIT), Ankara, Turkey, 2019, pp. 1-5, doi: 10.1109/ISMSIT.2019.8932895.

[12] Shi K., Yuan J., Lu Z., Xiao Y., and Hao Y., "Research on Information Convergence Processing and Transmission Method for Virtual Power Plant," in 2022 5th International Conference on Circuits, Systems and Simulation (ICCSS), Nanjing, China, May 2022, pp. 182–186. doi: 10.1109/ICCSS55260.2022.9802247.

Research Article

DESIGN IMPROVEMENT OF A 2 MVA SYNCHRONOUS MACHINE BY USING PARTICLE SWARM OPTIMIZATION

Kıvanç DOĞAN*¹ ⓘ, Ahmet ORHAN ² ⓘ

¹Fırat University, Electrical Electronics Engineering, Elazığ, Turkey
2 Fırat University, Electrical Electronics Engineering, Elazığ, Turkey
* Corresponding author; kivanc.dogan@firat.edu.tr

Abstract: *In this article; The step-by-step design of a 3-phase salient synchronous generator and efficiency optimization with particle swarm optimization technique are investigated. Unlike other studies in the literature, a system has been studied to minimize mathematical equation errors by using specific loading parameters that simplify the design process. It has been tried to obtain a program structure that minimizes programming problems by minimizing the number of variables used in the design. With the optimization of the specific loading parameters, the effects on the machine volume, cost and efficiency were examined. As a result, it has been observed that the productivity value increased with particle swarm optimization. In addition, the decrease in machine volume provided an advantage in terms of cost.*

Keywords*: sycnchronous machine, machine design, particle swarm optimization*

1. Introduction

Synchronous machines are widely used in power generation besides industrial applications in general Hydroelectric power plants are the most widely used area in power generation. They are used as round-pole high-speed turbo alternators in thermal power plants. It has also been used in wind power plants in recent years [1]. Synchronous generators are electrical machines that are mostly preferred to provide high capacity power generation and produced at different power levels from a few kVA to hundreds of MVA [2]. Synchronous generators are divided into two types which are salient-pole and round-pole synchronous generators based on their polar structures. Salient pole synchronous generators are generally used in hydroelectric power plants. They are preferred in low speed and high power applications. The aim of the design is to achieve maximum performance with minimum cost. However, providing minimum loss at low cost is one of the most important parts of the design. Simply minimizing the cost can result in high maintenance costs for the machine thus, the losses increase. For these reasons, there must be a balance between the cost and losses for the optimum design of the machine taking into account the application area [3]. Design optimization of electrical machines consists of two stages: design and optimization. In the design phase, the aim is to find the appropriate schema by searching for multidisciplinary analyzes or designs. In the optimization phase, the aim is to improve the performance of the proposed machine in the design phase with optimization methods. [4]. In this study, the efficiency of a three-phase generator is optimized by using the Particle Swarm Optimization (PSO) technique. In the study of Elez et al., optimization method for slot skew was applied in order to reduce damper bar losses and reduce total harmonic distortion of line voltage in salient pole synchronous generator. It has been concluded that with this optimization method, the damper bar losses can be reduced by 7 times and the total harmonic distortion can be reduced below 1%. [5]. In [1], the shape of the rotor is optimized to facilitate the assembly of excitation windings. The new rotor shape has greatly reduced the maintenance and repair costs of the synchronous machine [1]. The parameter calculation and specific loading options used in the design are also utilized in the compatibility design study of Oo and Thant's round-pole

synchronous generator. In this study conducted in 2019, they examined the relationship between the parameters that would improve the design by using specific loading options [6]. In another study [7], an optimization method is proposed to increase the efficiency of a salient pole synchronous generator using simulated annealing algorithm. Bell and Anpalahan optimize the rotor design in their works with the limitations placed on the main rotor geometry of a dislocated pole synchronous generator [8]. As a result of this optimization, the reducing effect on the total cost is observed. In [9], the topology of the shock absorber winding is investigated to increase the general performance of a 4 MVA salient-pole synchronous generator using conventional shock absorber winding. In this research, general algorithm optimization is used for improvement by performing finite element analysis [9].

Unlike the other studies in this paper, specific loading choices that simplify the design process are explained. Complex mathematical equations are avoided by specific loading selections. Here, PSO has been carried out by considering the parameter limits of the salient-pole synchronous machine.

2. Design of a synchronous generator

The designs of the salient pole generators are different from each other based on their power and usage areas. The design process usually starts with the calculation of the main dimensions. The first dimension to be chosen in the design is specific loading. The choice of specific electrical load, which is an empirically determined magnitude, varies between 20.000 A/m and 50.000 A/m for salient-pole synchronous machines, and between 50.000 A/m and 100.000 A/m for turbo generators [10]. Specific magnetic loading selection, which is an empirically determined magnitude, varies between 0.52 wb/m^2 and 0.65 wb/m^2 for salient-pole synchronous machines, while turbo generators range from 0.55 wb/m^2 to 0.65 wb/m^2 [11]. The inner diameter and axial length of the stator are the main dimensions of the machine. The parameters of the synchronous generator to be designed are given in Table 1.

Table 1. Parameters of synchronous generator

Parameter name	Variable	Value
Rated Power	kVA	2.000
Power Factor	-	0.8
Number of Poles	-	24
Rated Voltage	V	6.300
Frequency	Hz	50
Speed	rpm	250
Temperature	^{0}C	75

By using these values, the apparent power of the machine is obtained as follows

$$P_{sn} = C_0 \text{ x } D^2 \text{ x L x } n_s \tag{1}$$

where P_{sn} ; apparent power of the machine (kVA), C_0; utilization coefficient (kVA.dak/m^3), D ; stator inner diameter (m) and L ; the stator axial length(m). The synchronous speed of the machine is given by

$$n_s = \frac{120*f}{P} \tag{2}$$

where n_s, f, and p are the synchronous speed of the machine as rpm, frequency and the number of pole, respectively. The volume of the machine can be calculated from (1) as follows

$$D^2L = \frac{P_{sn}}{C_o \cdot n_s} \tag{3}$$

The stator inner diameter can be found by the following equation

$$D = \frac{V_a}{\pi.n_s} \tag{4}$$

where V_a is the circumferential speed. Its unit is m/s. The circumferential speed upper limit is 80 m/s for salient-pole synchronous machines [12].

Stator axial length is shown as follows

$$L = \frac{D^2 L}{D^2} \tag{5}$$

The total stator length must be 1 cm longer than the axial length so that the resulting flux remains between the stator and rotor as follows [13].

$$L_{top} = L + 0.01 \tag{6}$$

The net stator iron length is the length of iron remaining when five cooling channels whose wides are 1 cm are removed from the total length as follows [13]

$$L_i = L_{top} - (z_k * b_k) \tag{7}$$

where z_k and b_k are the number of the cooling channels and the cooling channel width whose value is usually taken as 1 cm, respectively [13]. The number of the cooling channels can be found by the following equation

$$z_k = \frac{L_{top}*10^{-2}*5}{6} \tag{8}$$

b_k in equation (7) is the width of the cooling channel. Usually its value is taken as 1 cm.
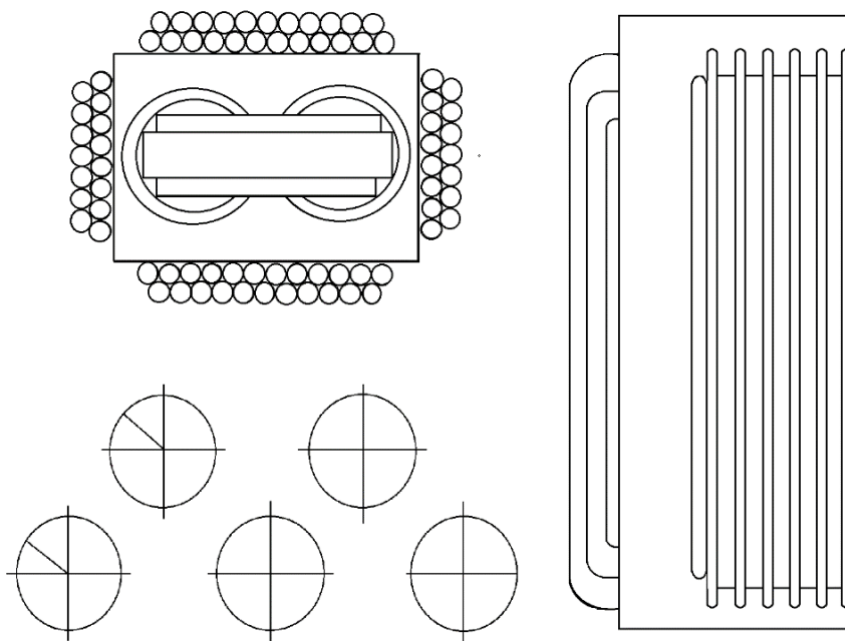
Figure 1. Detailed representation of the cooling channels [14].

The length of the air gap between the rotor and the stator is an important parameter that greatly affects the performance of the machine. Air gap length; depending on the pole step, it can be expressed by equation (10) [10].

$$\tau = \frac{\pi*D}{p} \tag{9}$$

$$l_g = (0.012\sim0.016) * \tau \tag{10}$$

where τ ; pole pitch (m), p ; the number of the poles, l_g; length of the air gap (m).

Another parameter that affects the performance of the machine is the number of slots. The correct selection of the slot number also affects the cost of the machine. Therefore, it is necessary to pay attention to the selection of the number of slots per phase pole. Generally, the number of slots per phase pole is taken between 3 and 4 for salient pole synchronous machines [10].

$$N_s = m * p * q \tag{11}$$

where N_s is total number of slot. Slot step y_s (m) value is shown by

$$y_s = \frac{\pi*(D+2*l_g)}{N_s} \tag{12}$$

There are boundary conditions for the slot step. These are given as follows:

$y_s \leq 25 \ mm$ for low voltage machines, $y_s \leq 40 \ mm$ for machines up to 6 kV, and $y_s \leq 60 \ mm$ for machines up to 15 kV [10]. The flux density in the teeth should not exceed 1.8 T. The slot width should not be less than 6 mm due to the production reasons.

$$b_o = y_s * 0.4 \tag{13}$$

where b_o (m) is the slot width.

$$A_{slot} = \frac{6*W_a*I_{phase}}{N_s*K_{fill}*j_s} \tag{14}$$

where $A_{slot} \ (m^2)$, W_a, I_{phase} (A), N_s, K_{fill}, and j_s (A/mm^2) are the slot area, the number of turns per current path, phase current, the number of the slot, the slot filling factor, and the stator current density, respectively. K_{fill} is an empirical expression and can be taken between 0.35 and 0.6. Slot height is a

$$h_s = \frac{A_{slot}}{b_o} \tag{15}$$

The slot height can be defined by adding the rim height to be taken as 5 mm [12]
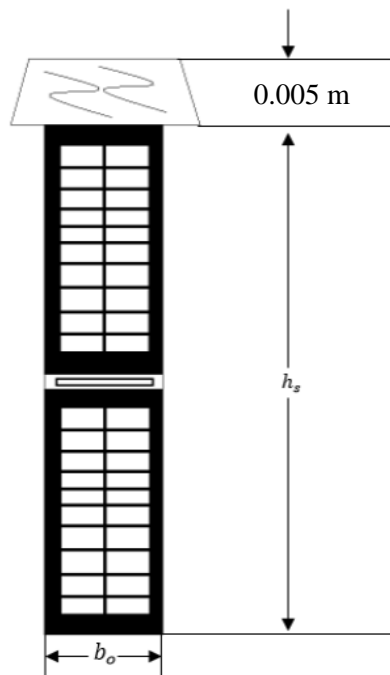
$$h_o = h_s + 0.005 \tag{16}$$

Figure 2. Slot width and height [13].

Stator yoke height is shown by

$$h_{ys} = \frac{B_g}{B_{ba}} * \frac{\tau}{\pi} \tag{17}$$

where B_g (T) and B_{ba} (T) are the flux densities in the air gap and stator yoke, respectively. B_g is taken in the range 0.8 to 1.05 T for salient-pole machines [12]. B_{ba} is also taken as 1.08 T [13]. The stator yoke height is used to calculate the stator outer diameter (D_s).

$$D_s = D + 2 * h_o + 2 * h_{ys} \tag{18}$$

In the design process, another parameter to be considered is the stator and rotor current densities. High current density means lower conductor, lower cost, higher temperature, more copper loss and lower slot area. The current density of the stator conductor is chosen between 3 A/mm^2 and 5 A/mm^2, and the current density of the rotor conductor is between 3 A/mm^2 and 6 A/mm^2. The cross-sectional area current density of the stator conductors can be calculated from the phase current value.

$$as = I_{phase}/j_s \tag{19}$$

where I_{phase} is the phase current and j_s is the current density. The cross-sectional area current density of the rotor conductors is calculated from its value as seen in equation (20).

$$af = I_f/j_r \tag{20}$$

where I_f is the field current and j_r is the rotor current density. Total number of the conductors in the stator is shown as follows

$$Z = \frac{\pi * D * ac}{I_{phase}} \tag{21}$$

The number of the conductors in one slot is also calculated by

$$Z_o = \frac{Z}{N_s} \tag{22}$$

where Z_o must be an integer value and be between 10 and 13 on the 2 MVA machine under consideration [13].

The design is completed by calculating the efficiency of the machine. The losses of the machine are considered in the efficiency calculation. These losses are as follows:

- Stator copper losses
- Rotor copper losses
- Additional losses due to the construction parts between the facade connections
- Iron losses
- Iron loss in teeth
- Pole foot surface losses
- Friction losses

The efficiency can be expressed by using the losses as follows

$$\eta = \frac{P_o}{P_o + P_T} \tag{23}$$

where P_o is the output power and P_T is the total losses.

3. Particle swarm optimization method

Optimization is the process of obtaining the most reasonable result by observing certain limitations for some objectives. It is an idea development tool. The goal of the optimization is always to achieve the best. One of the methods used in solving the optimization problems is Particle Swarm Optimization (PSO). PSO is an optimization method introduced by Kenedy and Eberhart in 1995 based on the movement of fish and insects as flocks [15]. It has been observed that the random actions of the animals moving in herds enable them to reach their goals more easily in some situations such as food and safety. PSO is based on the social information sharing between the individuals [16]. PSO which is an algorithm influenced by herd intelligence has been used for the optimization problems in various fields such as electromagnetics, design systems, manufacturing, and electrical power systems [17]. It is

also a method used in the control of nonlinear systems. It gives successful results when applied to the systems with many parameters and multivariate [18]. Each of the individuals in the PSO has a different speed value. At each step, individuals renew their speed values according to the individual in the best position [19]. Position and velocity vectors are expressed as $(x_{i1}, x_{i2}, \dots, x_{iD})$ and $V_i = (v_{i1}, v_{i2}, \dots, v_{iD})$, respectively. Each particle updates its position and speed based on its best position (pbest) and the best position of the whole cluster (gbest). After finding the best two values in each step, it updates itself according to the following equation [15]:

$$v_{id}{}^{t+1} = w * v_{id}{}^t + c_1 * r_1 * \left(pbest_{id}{}^t - x_{id}{}^t\right) + c_2 * r_2 * \left(gbest_{id}{}^t - x_{id}{}^t\right) \qquad (24)$$

$$x_{id}{}^{t+1} = x_{id}{}^t + v_{id}{}^{t+1} \qquad (25)$$

where $i = 1, 2, \dots, NP$ and NP, w, c_1 and c_2 are scaling factors. NP determines the size of the flock, w is the inertia weight value for each iteration, c_1 and c_2 are the relative influence of the cognitive and social components, respectively. r_1 and r_2 are any random numbers in the range between 0 and 1. $x_{id}{}^t$, $v_{id}{}^t$, $pbest_{id}{}^t$ are the position, speed and personal best values for d. position in size of t. iteration of the i. particle, respectively. Under the same conditions, the best particle of the whole flock is $gbest_{id}{}^t$. In this study, c_1 and c_2 learning factors are taken randomly to achieve better performance of the optimization.

Since there is no need for derivative information in PSO, it differs from the other optimization techniques. PSO is also easy due to the small number of the parameters that need to be adjusted compared to the other algorithms [20].

The parameters of the PSO applied in this study are given in Table 2.

Table 2. PSO Parameters

Parameter name	Variable	Value
Cognitive component	c_1	0.12
Social component	c_2	1.2
No. of particles	n	100
No. of iterations	NP	1000
Minimum inertia weight	w_{min}	0.4
Maximum inertia weight	w_{max}	0.9
Dimension	dim	3

4. Optimization of the synchronous generator

Before the optimization process, the efficiency value of the synchronous generator was calculated as 94.63%. Efficiency was chosen as the target parameter while optimizing. PSO method is preferred for the optimization. The limits of the parameters that will affect the efficiency are determined for the optimization process. In this study, the limiting parameters and limits are given in Table 3.

Table 3. Some parameters affecting the efficiency and their ranges.

Parameter	Their ranges

B_{av}	0.52 wb/m^2-0.65 wb/m^2
ac	20,000 A/m -50,000 A/m
V_a	30 m/s -80 m/s

Along with these limits, the optimization process is realized by considering the values of the scaling factors. The values of the c_1 and c_2 learning factors are taken as 0.12 and 1.2, respectively. As a result of the optimization process, the efficiency of the machine reached to 94.84%. The efficiency graphics are given before and after the optimization process in Figure 3 and 4, respecively.
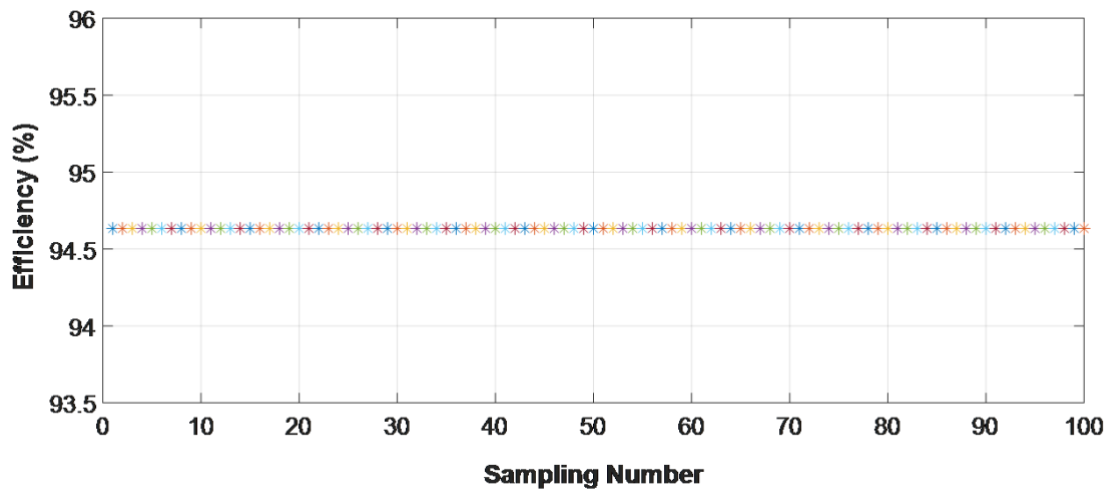

Figure 3. The efficiency of the synchronous generator before the optimization.
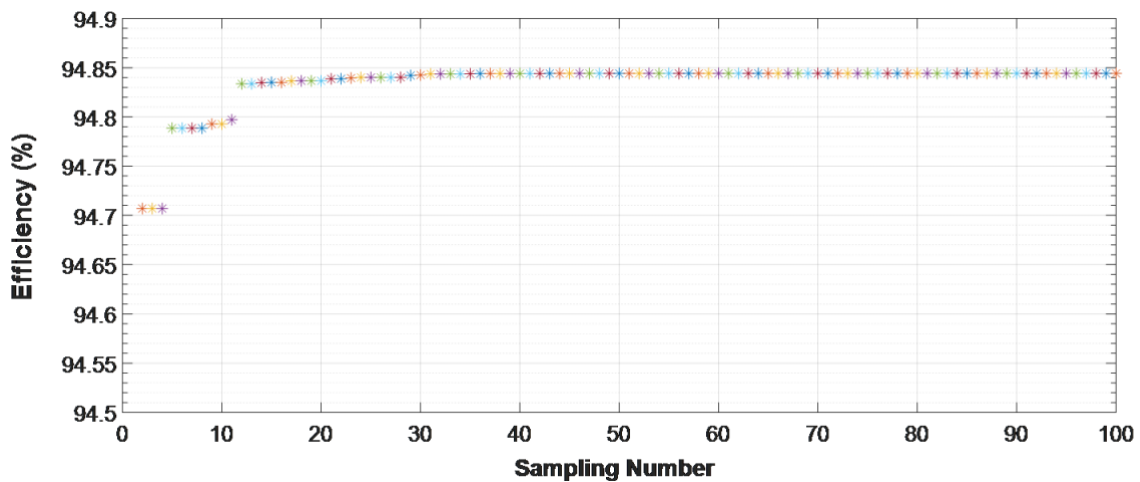

Figure 4. The efficiency of the synchronous generator after the optimization.

In addition to the improvement in efficiency with the optimization process, B_{av}, ac, V_a, pole step, number of turns per phase and total loss values are also optimized. The values of the parameters before and after optimization are given in Table 4.

Table 4. Optimized parameter results

Parameters	Pre-Optimization Value	Post Optimization
B_{av} (wb/m^2)	0,52	0,55
ac (A/m)	43850	43720
V_a (m/s)	31,5	30,79
Pole pitch (m)	0,315	0,307
The number of turns per phase	305	295
Total losses (W)	90729	86978
Efficiency (%)	94,63	94,84

5. Conclusions

In this paper, the design calculation of a 2 MVA synchronous machine has been made. The designed synchronous machine has been optimized by PSO method. Unlike the other studies in the literature, the complexity of the mathematical expressions in the design process is removed by using specific loading selection parameters in this work. In this way, the design of the synchronous machine to be used according to the application area can be expressed more clearly. In addition, optimization was applied to specific loading parameters. By optimizing the machine, the B_{av} value has changed, increasing the steady state stability. The change of ac value also reduces the copper losses, stray load losses and the number of armature conductors. On the other hand, the change in the value of the pole pitch provides the air gap length, pole body width and yoke height to decrease. Besides with the decrease in the number of the windings per phase, the volume of the machine also reduces. As a result, it is seen that the reduction in the volume of the machine provides a cost benefit. With the increase in the efficiency value, the intended purpose of the design is achieved.

References

[1] Yuan,T., Yang, N., Zhang, W., Cao, W., Xing, N., Tan, Z., Li, G. "Improved synchronous machine rotor design for the easy assembly of excitation coils based on surrogate optimization", Energies, 11(5), 1311, 2018.

[2] Varan, M., Oylek, I., Dereli, S., "Üç fazlı senkron bir makinenin değişken yük durumları için geçici hal sonlu eleman analizi", Gaziosmanpaşa Bilimsel Araştırma Dergisi, *6*(özel sayı (ısmsıt2017)), 59-72, 2017.

[3] Upadhyay, K. G., Design of Electrical Machines, New Age International, 2011.

[4] Lei, G., Zhu, J., Guo, Y., Liu, C., & Ma, B. "A review of design optimization methods for electrical machines", Energies, 10(12), 1962, 2017.

[5] Elez, A., PetriniC, M., PetriniC, M., Vaseghi, B., Abasian, A. "Salient pole synchronous generator optimization by combined application of slot skew and damper winding pitch methods", Progress in electromagnetics research M, 73, 81-90, 2018.

[6] Oo, T.Z., Thant A.M., "Compatibility design of non-salient pole synchronous generator", International Journal of Trend in Scientific Research and Development, 3(4), 2019.

[7] Udema, S., Fraeger, C. "Design of a Highly Efficient Electrical Excited Salient-Pole Synchronous Machine Utilizing an Optimization Algorithm" In: Innovative Small Drives and Micro-Motor Systems 11th GMM/ETG-Symposium, (pp. 1-6), 2017.

[8] Bell, A. E., Anpalahan, P., "Optimisation of salient-pole rotor for synchronous generators", In: IEEE 2018 XIII International Conference on Electrical Machines (ICEM), pp. 339-344, 2018.

[9] Nuzzo, S., Degano, M., Galea, M., Gerada, C., Gerada, D., Brown, N., "Improved damper cage design for salient-pole synchronous generators", IEEE Transactions on Industrial Electronics, 201664(3), 1958-1970, 2016.

[10] Nagarajan V. S., Rajini V., Electrical Machine Design, Pearson, 2018.

[11] Shanmugasundaram, A., Gangadharan, G., Palani R., Electrical Machine Design Data Book, New Age Intenational Pvt. Ltd., 2007.

[12] Boldea, I., Synchronous generators, CRC press, 2015.

[13] Boduroğlu, T., Elektrik Makinaları Dersleri. 3(2), Senkron Makinaların Hesap ve Konstrüksiyonu, İTÜ Matbaası, İstanbul, 1994.

[14] Ateş, H., Elektrik Makinalarının Hesabı, Yüksek Teknik Öğretmen Okulu Matbaası, Ankara, 1975.

[15] Eberhart, R., Kennedy, J., "Particle swarm optimization", In Proceedings of the IEEE International Conference on Neural Networks, 4, 1942-1948, 1995.

[16] Ozsağlam, M.Y., Cunkas, M., "Optimizasyon problemlerinin çözümü için parçaçık sürü optimizasyonu algoritması", Politeknik Dergisi, 11(4): 299-305, 2008.

[17] Dal, O., Yıldırım, M., Kurum, H., "Optimization of permanent magnet synchronous motor design by using PSO", In: 4th IEEE International Conference on Power Electronics and their Applications (ICPEA), pp. 1-6, 2019.

[18] Berber, O., Ateş, M., Alhassan, H.A., Güneş, M., "Parçacık sürü optimizasyonu ve PID ile mobil robotun optimum yörünge kontrolü", Kahramanmaraş Sütçü İmam Üniversitesi Mühendislik Bilimleri Dergisi, 19(3): 165-169, 2016.

[19] Ozsağlam, M.Y., Parçacık sürü optimizasyonu algoritmasının gezgin satıcı problemine uygulanması ve performansının incelenmesi, Master's Thesis, Selçuk Üniversitesi Fen Bilimleri Enstitüsü, Konya, 2009.

[20] Cavuslu, M.A., Karakuzu, C., Sahin, S., "Parçacık sürü optimizasyonu algoritması ile yapay sinir ağı eğitiminin FPGA üzerinde donanımsal gerçeklenmesi", Politeknik Dergisi, 13(2), 83-92, 2010.

Research Article

DESIGN OF PERTURB AND OBSERVATION AND FUZZY LOGIC BASED MPPT CONTROLLERS OF PV ARRAY BY USING POSITIVE SUPER LIFT DC/DC BOOST CONVERTER

Ayse KOCALMIŞ BİLHAN*1 [iD] *, Serenay EMİKONEL 2* [iD]

1 Nevsehir Haci Bektas Veli University, Faculty of Engineering, Department of Electrical Electronic Engineering, 50200, Nevsehir, Turkey
2 Nevsehir Haci Bektas Veli University, Faculty of Engineering, Department of Electrical Electronic Engineering, 50200, Nevsehir, Turkey
*Corresponding author; akbilhan@nevsehir.edu.tr

Abstract: *The electricity which is generated from the photovoltaic (PV) module needs a couple of requirements for utilizing. Firstly, the PV module should work in maximum power point, and secondly, it is needed a power conversion unit. To calculate to Maximum Power Point (MPP) of a PV module or array, solar radiation, ambient temperature, cloudiness ratio, and even wind speed have to be considered. In this paper, the duty cycle of the power conversion unit has been calculated by considering solar radiation. In these calculations, a conventional method which is perturb and observation (P&O), and another approach which is fuzzy logic control (FLC) were studied and compared by using MATLAB/Simulink.*

Keywords: *converter, fuzzy logic, perturb and observation, solar energy*

1. Introduction

With the increase in energy demand, electrical production from fossil-based energy sources brings with it many problems such as global warming, environmental pollution, air pollution, and health threats [1-4]. The fact that these energy sources which will be consumed away in the next century have led researchers to investigate renewable energy sources. In this respect, solar energy, wind energy, water energy, bioenergy and their applications have become more popular energy research topics [5-8]. Solar energy becomes one of the most popular energy sources of electrical power generation in renewable energy sources. However, today, the high initial installation costs of PV systems and the fact that only a small part of the rays from the sun can be converted into electrical energy is the most important problem of PV systems.

The DC output voltage which is directly obtained from the solar module is usually low. Therefore, it needs to be boosted a to higher DC voltage to meet the load or it can be converted to AC voltage. Also, because the energy production capacities of PV systems change at any time depending on temperature and radiation and it is desired to obtain high efficiency from PV systems, these systems must be operated at the maximum power point. Despite the changing environmental conditions, various MPPT algorithms such as perturb and observation (P&O), fuzzy logic, particle swarm optimization, etc. have been developed in the literature to keep the amount of energy produced from solar energy at a high level [9]. The perturb and observation algorithm (P&O) is a widely used method for tracking the maximum power point in both solar and wind energy, due to its simple feedback structure, and low cost and ease of implementation. Also, in recent years, fuzzy logic-based controllers became more popular for MPPT [10]. In many recent research, in order to increase the efficiency of PV systems, the fuzzy logic method has been integrated into the traditional P&O method [11].

In PV energy systems, various converter circuits such as buck, boost, or buck-boost are used to provide a constant voltage with the desired amplitude to the load or the inverter. The proposed system contains a control system, solar array, a DC/DC converter, and load. In Fig. 1, the output voltage of the PV module is regulated and increased by using DC/DC positive lift boost converter circuit [12, 13]. The super-lift technique is the popular method widely used for boosting the voltage. It can be obtained higher output voltage value than input voltage value by using a lift boost converter circuit. A solar array has two inputs irradiance (G) and temperature (T).
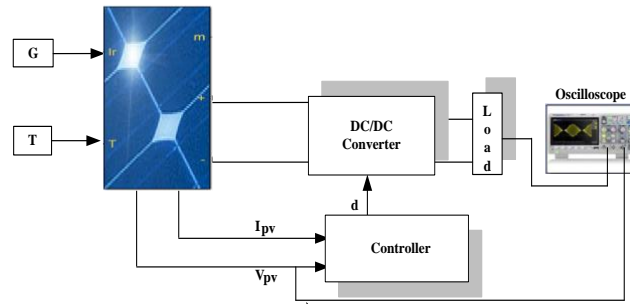

Figure 1. Block diagram of the whole system

The paper is arranged as follows: Section II covers the positive super lift DC/DC boost converter. In Section III, the studied system and both P&O and FLC-based MPPT techniques are detailed. The simulation results are presented and discussed in Section IV. Finally, conclusions are provided in section V.

2. Positive super lift boost converter

The positive super lift converters have very high efficiency among DC converters and it is aimed to raise the voltage without ripple by using these types of converters [14]. The output voltage increases in geometric progression stage-by-stage. This type of converter can be separated into two part such as the main circuit and the additional circuit. The circuit gain can be increased with each additional circuit. The proposed system consists of one switching component (S), 2 capacitors, one inductor, 2 fast recovery diodes, and R load. The equivalent circuit has been shown in Fig. 2.
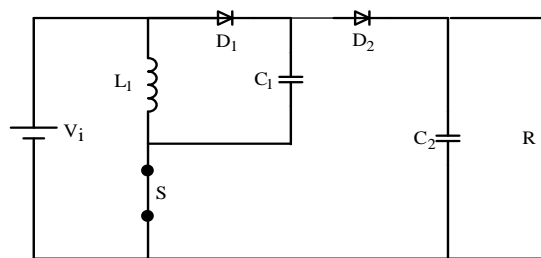

Figure 2. The positive super lift converter circuit

The switch-on (turn-on) & switch-off (turn-off) equivalent circuits are shown in Fig.3 (a) and (b), respectively.
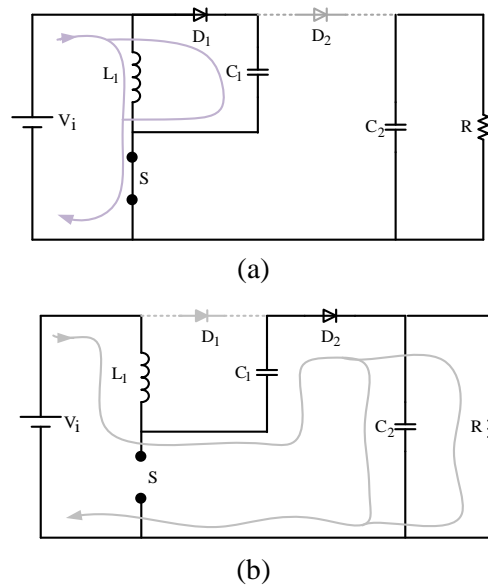
(a)

(b)

Figure 3. (a) Equivalent circuit diagram during the switch-on period; (b) Equivalent circuit diagram during the switch-off period.

The voltage across capacitor C_1 increase to V_i during the turn-on duration. The current flowing through the inductance L_1 increases with the current i_{L1} and the input voltage V_i during the conduction period dT. The input current i_i is equal to $i_{L1} + i_{C1}$. In the turn-off duration $((1-d)T)$, D_1 is reverse biased and turns off, and D_2 turns on. During the turn-off time of the switch (S), the input current is equal to i_{L1} ($i_{L1}=i_{C2}$). Therefore the ripple of the inductor current i_{L1} and output voltage (V_o) can be calculated as;

$$\Delta i_{L1} = \frac{V_i dT}{L_1} = \frac{V_0 - 2V_i(1-d)T}{L_1} \tag{1}$$

$$V_0 = \left(\frac{2-d}{1-d}\right)V_i \tag{2}$$

3. Mppt control methods

To increase the efficiency obtained from photovoltaic (PV) modules, these modules are required to operate at the maximum power point. Many theories such as perturb and observation (P&O), fuzzy logic (FL), pulsating conductivity (IC), and data mining are applied in the literature to determine the maximum power point by considering the radiation value. Figure 1 shows the block diagram of the system used during this study.

3.1. The perturb and observation algorithm *(P&O)*

Due to its ease of application, the perturb and observation algorithm (P&O) is one of the most preferred methods for Maximum Power Point Tracking (MPPT). The algorithm works iteratively until the maximum power point is determined [15, 16]. There are multiple possibilities for the P&O algorithm in the literature, but the classical flow chart of the P&O algorithm is given in Fig. 4.
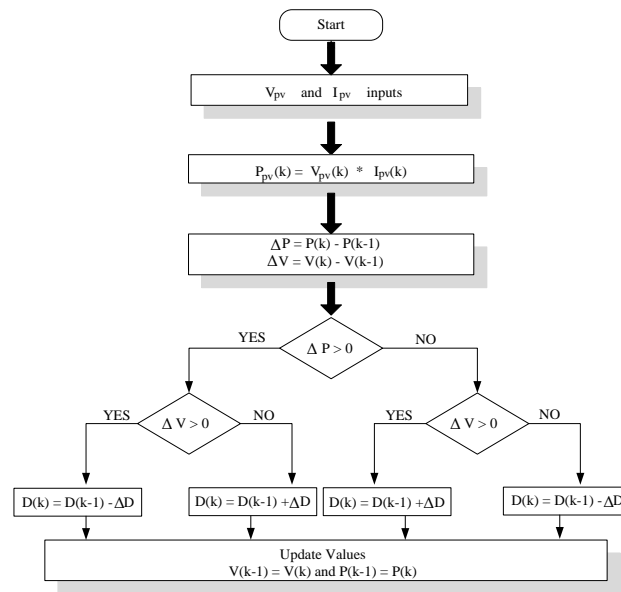
Figure 4. Flow Chart of P&O Algorithm

When the flow chart is examined, it can be observed that the voltage and current are selected as the initial value. The power of the PV module is calculated by using these values. During continuous operation, an instantaneous power value is calculated using the current (I) and voltage (V) information obtained with the help of sensors. By comparing this power value with the previous power value, the power change is calculated (ΔP). Also, when calculating the power change, the change in the voltage (ΔV) and the change in current (ΔI) are calculated. MPPT is performed with these calculated values. While making this determination; if the ratio is bigger than 0, the operating point is the left of the maximum power point, if the ratio of is lower than 0, the operation point is the right of the maximum power point, and if the ratio of is equal to 0, the operating point is at the maximum power point. This situation is illustrated in Fig. 5.
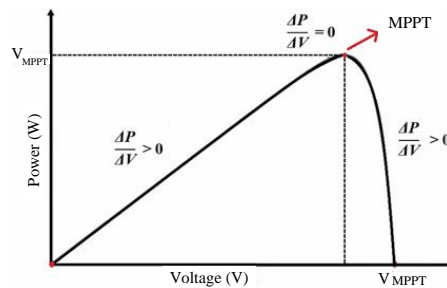

Figure 5. P&O Algorithm

The duty ratio of the positive super lift converter is controlled by the output of the P&O algorithm which has been shown in Fig. 6.
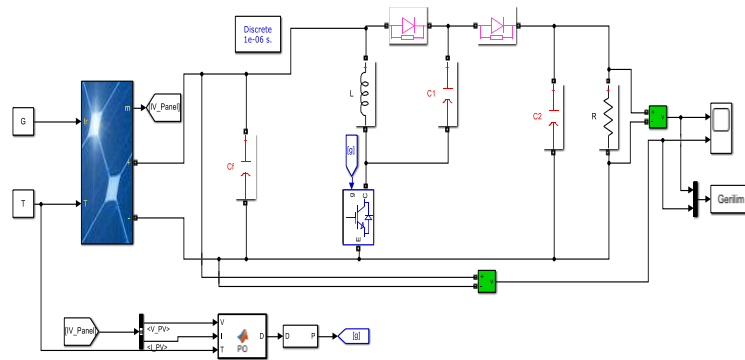
39

Figure 6. The MPPT tracking with P&O

3.2. The fuzzy logic control (FLC) algorithm

The use of fuzzy logic controllers in a PV system has significant increase year by year. In particular, FLC has become popular due to its superior ability to deal with the nonlinearity and uncertainties of any system and its easy design. Also, it has expanded its use in PV system applications because it is durable and does not require full knowledge of the system model compared to other control methods [17].

In this study, the power change was obtained by calculating the power with the current and voltage information coming from the PV panel and subtracting it from the previous power value, and the error (e) and error change (de) inputs produced by the panel, based on the voltage changes obtained by subtracting the current voltage from the previous voltage value, membership transforms it into linguistic variables with functions. The flow chart of FLC MPPT method has been shown in Fig. 7 [18,19].
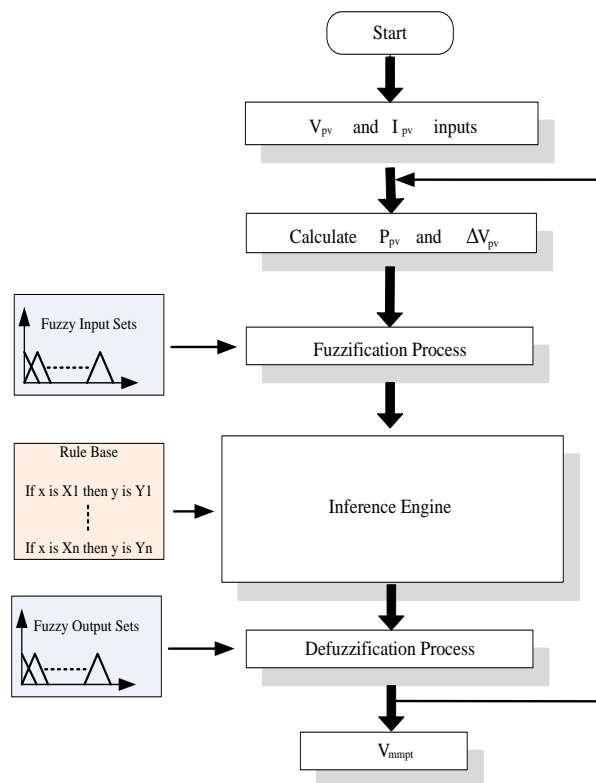

Figure 7. Flow chart of FLC Algortihm

To implement the MPPT algorithm, the fuzzy logic designer function from MATLAB has been used. The controller's inputs are error (e) and variations in error (de) are calculated by using Eq.(3) and (4) [20]:

$$e = \frac{P(k) - P(k-1)}{V(k) - V(k-1)} \tag{3}$$

$$de = e(k) - e(k-1) \tag{4}$$

In this study, Mamdani's approach has been used as the fuzzy inference technique. In this technique, it is based on the max-min conditions. Also, triangular curves as fuzzy membership functions (MFs) have been used. Five MFs are used for better accuracy; however, it takes more processing time and demands more memory. The linguistic variables which are shown in Fig. 8 are denoted as NB (negative big), NS (negative small), ZE (zero), PS (positive small), and PB (positive big). The developed 25 rules are given in Table I.
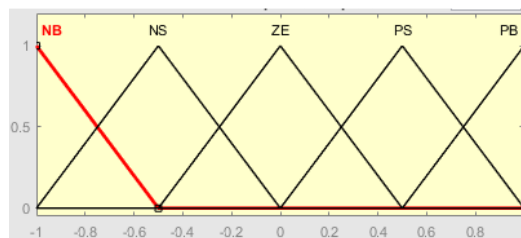

Figure 8. The FLC membership functions

Table 1. Fuzzy rules tables

e/de	NB	NS	ZE	PS	PB
NB	NB	NB	NS	NS	ZE
NS	NB	NS	NS	ZE	PS
ZE	NS	NS	ZE	PS	PS
PS	NS	ZE	PS	PS	PB
PB	ZE	PS	PS	PB	PB

The duty ratio of the converter is controlled by FLC. The maximum power point of solar array which is used fuzzy logic algorithm has been shown in Fig. 9.
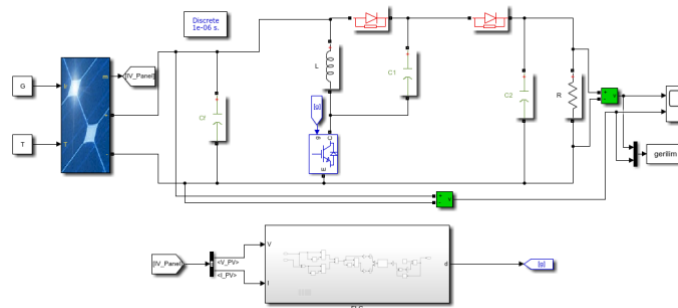

Figure 9. The MPPT tracking with FLC

4. Design and simulation results

The electrical characteristics of a PV module that have been used, given by the manufacture's data sheet at the nominal temperature of 25°C and average solar spectrum at AM 1.5, are shown in Table II.

Table 2. Electrical Characteristics of LNSE-245P PV Module

Optimum Operating Voltage (V_{mp})	30V
Optimum Operating Current (I_{mp})	8.7A
Open Circuit Voltage (V_{oc})	37.1V
Short Circuit Voltage (I_{sc})	8.74A
Max. Power (P_{max})	245W

In the simulation, 5 series modules connecting 2 parallel strings have been used. In Fig. 10, Power-Voltage (P_{pv}/V_{pv}) and Current-Voltage (I_{pv}/V_{pv}) curves have been shown.
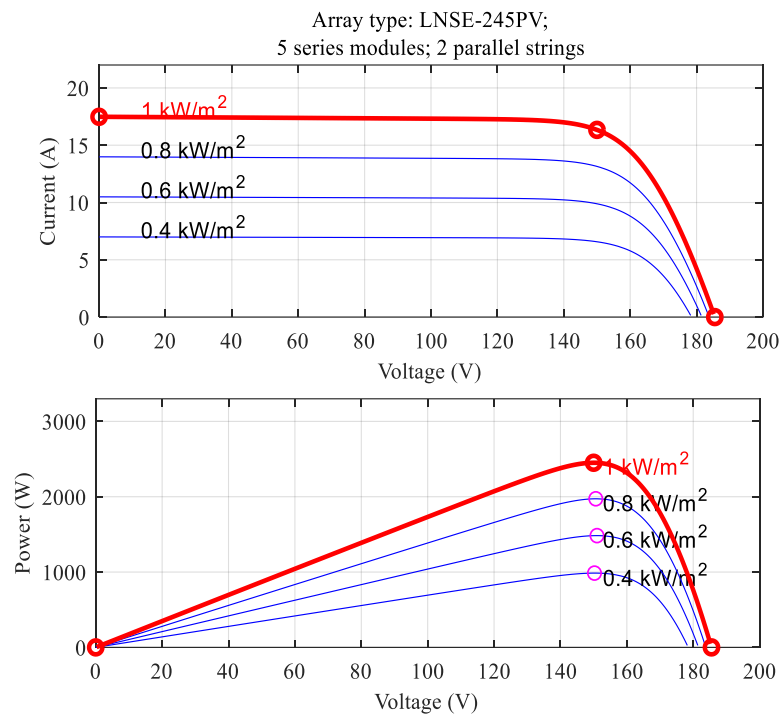

Figure 10. Caracteristiques of the PV array

Simulation results have been taken under various irradiance conditions such as 1000 W/m², 800 W/m², and 600 W/m². The parameters of the DC/DC converter are used as C_f=4400µF, C_1=C_2=2200µF, L=10mH, and R=80Ω.
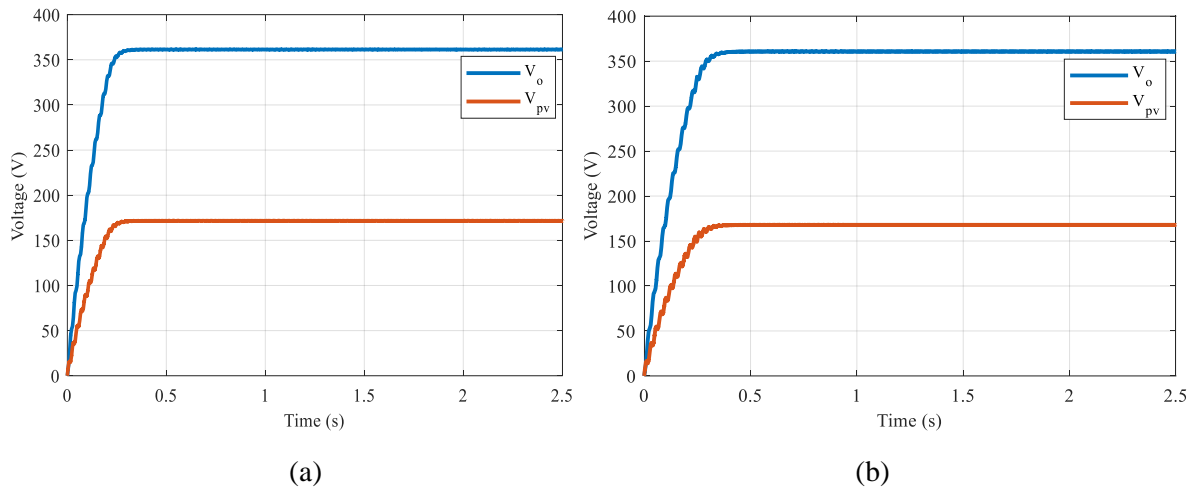
Figure 11. Simulation results for (a) P&O controller, (b) FLC for 1000 W/m^2 irradiance value

Fig. 11 (a) and (b) show the simulation results for both P&O and FL controllers with 1000 W/m^2 irradiance value, respectively. In the Figures, V_o represents the output voltage value of DC/DC converter and V_{pv} represents the output voltage value of PV array.

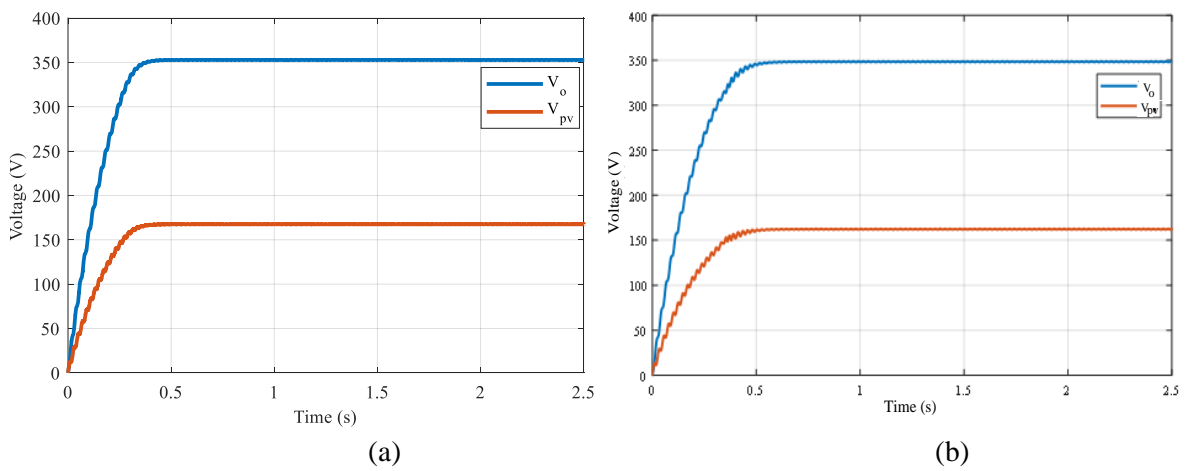In Fig. 12, the simulation results were obtained with 800 W/m^2 irradiance value.

Figure 12. Simulation results for (a) P&O controller, (b) FLC for 800 W/m^2 irradiance value

The simulation results for 600 W/m^2 irradiance value for both P&O and FLC algorithms have been shown in Fig.13.
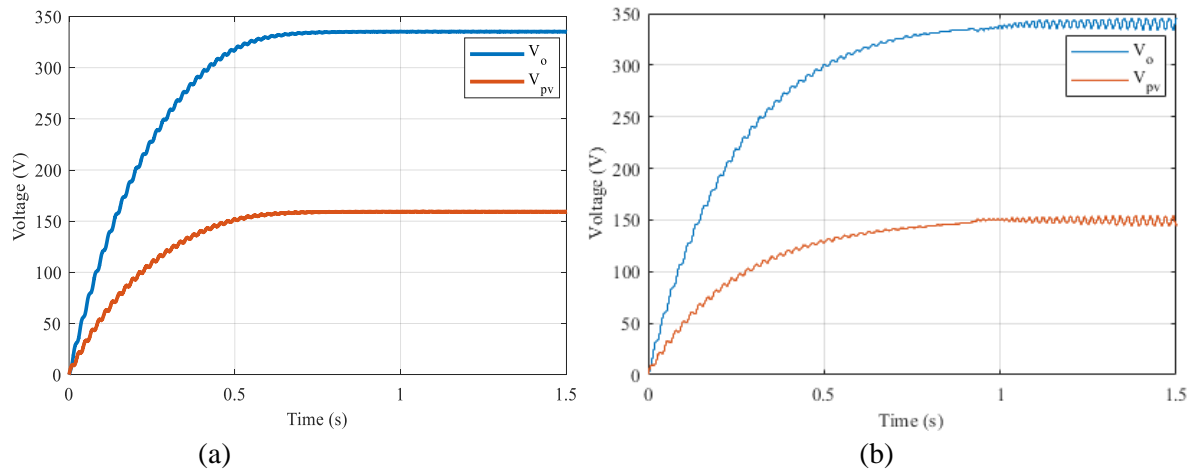

Figure 13. Simulation results for (a) P&O controller, (b) FLC for 600 W/m^2 irradiance value

In Fig. 14., the output voltage of PV, the output voltage of DC/DC converter with P&O controller, and the output voltage of DC/DC converter with FLC are given for 1000 W/m^2 irradiance value.
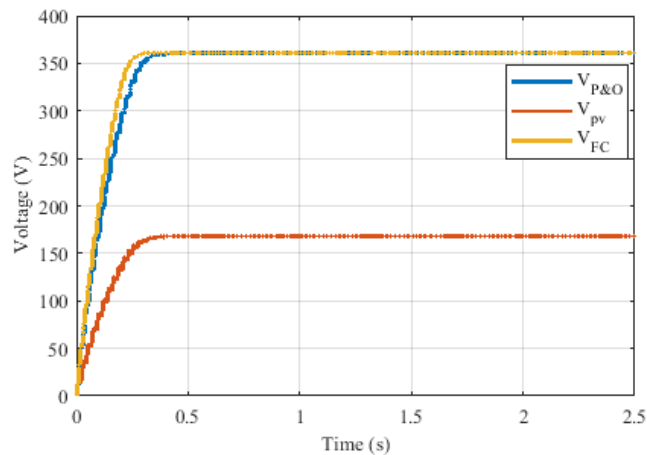

Figure 14. Simulation results of PV array and DC/DC converter for P&O controller and FL controller with 1000 W/m^2 irradiance value

5. Conclusion

The progressive decrease of fossil fuels and environmental concerns lead researchers to research other energy sources such as solar, wind, etc. In the literature, many various systems were designed to convert the irradiation coming from the sun into electrical energy. For this purpose, solar panels are highly preferred. In this work, the positive super lift converter and PV array has been modelled and designed by using MATLAB/Simulink simulation program. P&O and fuzzy logic methods were proposed and used to achieve to maximum power from photovoltaic array. It is aimed to achieve higher sensitivity and the fastest system responses to changes in irradiance and temperature levels by this work. Therefore, two different MPPT methods have been simulated and compared.

In the conventional DC/DC converter circuits, an increase of the voltage is carried out up to a certain limit, while in the positive super lift converter circuits, this situation enables higher values to be reached. For this reason, the positive super lift converter is used in this study. It is an advantageous situation for this circuit as it responds faster and reaches the desired maximum power point in a lower duty period. In this way, more energy can be transferred to the grid or higher voltage levels can be achieved for individual users.

As a result, it can be concluded that the FLC algorithm is very sensitive and consume significant computational resources. Also, it is seen that FLC based MPPT controller has better extraction of the maximum power from PV modules.

References

[1] W. Nsengiyumva, S. G. Chen, L, Hu, X. Chen, "Recent advancements and challenges in Solar Tracking Systems (STS): A review", Renewable and Sustainable Energy Reviews, 81, 250-279, 2018.

[2] Y. Zhu, J. Liu, X. Yang, "Design and performance analysis of a solar tracking system with a novel single-axis tracking structure to maximize energy collection", *Applied Energy*, 264 (114647), 2020.

[3] F. Dinçer, "The analysis on photovoltaic electricity generation status, potential and policies of the leading countries in solar energy", *Renewable and Sustainable Energy Reviews*, 15 (1), 713–720, 2011.

[4] J. Yu, Y.M. Tang, K.Y. Chau, R.. Nazar, S. Ali, W. Iqbal, "Role of solar-based renewable energy in mitigating CO_2 emissions: Evidence from quantile-on-quantile estimation", *Renewable Energy,* 182, 216-226, 2022.

[5] A. Rahman, O. Farrok, M.M. Haque, "Environmental impact of renewable energy source based electrical power plants: Solar, wind, hydroelectric, biomass, geothermal, tidal, ocean, and osmotic", *Renewable and Sustainable Energy Reviews*, 161, 2022.

[6] Z. Gumus, M. Demirtas, "Comparison of the algorithms used in maximum power point tracking in photovoltaic systems under partial shading conditions", *Journal of Polytechnic*, 24(3), 853-865, 2021.

[7] S.Adak, H.Cangi, B.Eid and A.S.Yilmaz, "Developed analytical expression for current harmonic distortion of the PV system's inverter in relation to the solar irradiance and temperature", *Electric. Eng.*, 1031, 103 (1), 697-704, Oct. 2020.

[8] C. Haydaroglu, B. Gumus, "Examination of web-based pvgis and sunny design web photovoltaic system simulation programs and assessment of reliability of the results", *Journal of Engineering and Technology*, 32-38, 2017.

[9] R.. Das, K.M. Rahman, "Effect of response time and starting point of duty cycle in maximum power point tracking operation of solar panel using PO algorithm," *2016 9th International Conference on Electrical and Computer Engineering (ICECE)*, 357-360, 2016.

[10] L. P. N. Jyothy and M. R. Sindhu, "An artificial neural network based mppt algorithm for solar pv system," in *2018 4th International Conference on Electrical Energy Systems (ICEES)*, 375–380, 2018.

[11] M. Zerouali, S. Zouirech, A.E. Ougli, B. Tidhaf, H. Zrouri, "Improvement of conventional mppt techniques P&O and INC by integration of fuzzy logic," *2019 7th International Renewable and Sustainable Energy Conference (IRSEC)*, 1-6, 2019.

[12] A.S. Tekade, R. Juneja, M. Kurwale, P. Debre, "Design of positive output super-lift luo boost converter for solar inverter," *2016 International Conference on Energy Efficient Technologies for Sustainability (ICEETS)*, 153-156, 2016.

[13] N. Silpa, J. Chitra, "An improved luo converter for high voltage applications," *International Journal of Emerging Technology and Advanced Engineering*, 4(5), May 2014.

[14] S.S. Dheeban, N.B. Muthu Selvan, L. Krishnaveni, "Performance improvement of Photo-Voltaic panels by Super-Lift Luo converter in standalone application", *Materials Today: Proceedings*, 37, 1163-1171, 2021.

[15] C.H. Basha, C. Rani, "Diferent conventional and soft computing mppt techniques for solar pv systems with high step-up boost converters: a comprehensive analysis", *Energies,*13(1), 371, 2020.

[16] M.A. Vildirim, M. Nowak-Ocłoń, "Maximum power point tracking algorithm under time-varying solar irradiation", *Energies,* 13, 6722, 2020.

[17] M. İ. Ort, "PV sistemlerde güneşi takip eden sistem tasarımı ve mppt kontrolu ile enerjinin yuke maksimum olarak aktarılması", *İstanbul Technical Uni., Fen Bilimleri Enst., MSs,* s. 52, Istanbul, 2016.

[18] T. L. Kottas, S. B. Yiannis, D. K. Athanassios "New maximum power point tracker for PV arrays using fuzzy controller in close cooperation with fuzzy cognitive networks" *IEEE Transactions on Energy Conversion,* 21(3), 793-803, 2016.

[19] M.A.A. Mohd Zainuri, M.M. Mohd Radzi, A.C. Soh, N. Rahim, "Adaptive P&O-fuzzy control mppt for pv boost dcdc converter." *2012 IEEE Int. Conf. on Power and Energy*, pp. 524-529, 2012.

[20] D. Haji, N. Genc, "Fuzzy and P&O Based MPPT Controllers under Different Conditions", *7th Int. Conf. on Renewable Energy Research and Applications (ICRERA),* 14-17 Oct., 649-655, 2018.